UNIVERSITAT POLITÈCNICA DE CATALUNYA
BARCELONATECH
Escola d'Enginyeria de Barcelona Est

MASTER'S THESIS

Master's degree in Chemical Engineering – Smart Chemical Factories

CARBON CAPTURE AND UTILIZATION FROM A MUNICIPAL SOLID WASTE-TO-ENERGY PLANT

Report and Annexes

Author: Pol Llorach Naharro
Director: César Alberto Valderrama Angel
Co-director: José Luis Cortina Pallás

Call for proposal: June 2021

Resum

Aquest treball proposa la captació i us del carboni a la planta de valorització energètica TERSA de Sant Adrià del Besós, Barcelona. Aquests processos, sota el paradigma de la economia circular, utilitzen el CO_2 dels gasos de combustió com a matèria primera, reduint les emissions de gasos d'efecte hivernacle i tancant la cadena de subministrament de l'empresa. La producció de bio-metà i de bicarbonat de sodi per a l'auto-consum dels forns i la línia de tractament de gasos àcids , respectivament, són els principals escenaris desenvolupats.

La captació de CO_2 amb tecnologia de membranes és la base per a ambdós escenaris. En el cas del bio-metà, aquest es produeix amb hidrogen verd, via electròlisi, i CO_2. D'altra banda, el bicarbonat de sodi es produeix a partir de carbonat de sodi i CO_2.

Els balanços de matèria i energia de cada escenari han sigut calculats per a dimensionar els principals equips de procés. Les despeses capitals (CAPEX) i els costos d'operació (OPEX) han sigut estimades utilitzant les dades tècniques obtingudes. A més a més, s'ha realitzat un anàlisi de sensibilitat per tal d'investigar quins elements tenen un pes més important dins dels costs totals.

Els resultats obtinguts són atractius i permeten a TERSA conèixer l'ordre de magnitud de la inversió necessària per a executar la proposta. En cas que aquest disseny conceptual fos considerat potencialment interessant des del punt de vista estratègic, el següent pas dins del cicle de vida del projecte seria el començament de la fase d'enginyeria bàsica o pre-FEED.

Resumen

Este trabajo propone la captura y utilización de carbono en la planta de valorización energética TERSA de Sant Adrià del Besós, Barcelona. Estos procesos, bajo el paradigma de la economía circular, usan el dióxido de carbono de los gases de combustión como materia prima, reduciendo las emisiones de gases de efecto invernadero y cerrando la cadena de suministro de la empresa. La producción de bio-metano y bicarbonato de sodio para el auto-consumo de los hornos y la línea de tratamiento de gases ácidos, respectivamente, son los principales escenarios desarrollados.

La captura de CO_2 con tecnología de membranas es la base para ambos escenarios. En el caso del bio-metano, éste se produce con hidrogeno verde, vía electrolisis, y CO_2. Por otro lado, el bicarbonato de sodio se produce a partir de carbonato de sodio y CO_2.

Los balances de materia y energía de cada escenario se calcularon para dimensionar los principales equipos de proceso. Los gastos en capital (CAPEX) y los costes de operación (OPEX) fueron estimados usando los datos técnicos obtenidos. Además, se realizó un análisis de sensibilidad para investigar qué elementos condicionan más los costes totales.

Los resultados obtenidos son atractivos y permiten a TERSA conocer el orden de magnitud de la inversión necesaria para llevar a cabo su implementación. En caso que este diseño conceptual fuera considerado de interés potencial estratégico, el siguiente paso del ciclo de vida del proyecto sería el comienzo de la fase de ingeniería básica o pre-FEED.

Abstract

This work proposes carbon capture and utilization in the TERSA waste-to-energy (WtE) plant, located in Sant Adrià del Besós, Barcelona. These processes, following the circular economy paradigm, use CO_2 from the flue gases as feedstock, reducing the greenhouse gases emissions while closing the supply chain of the company. The production of bio-methane and sodium bicarbonate for the self-supply in the furnaces and the acidic gases treatment line, respectively, are the main scenarios developed.

Membrane technology for CO_2 capture is the starting point for both scenarios. In the case of bio-methane, it is produced from green hydrogen, via electrolysis, and CO_2. On the other hand, sodium bicarbonate is produced from sodium carbonate and CO_2.

Mass and energy balances were calculated to size up the process equipment. Capital expenses (CAPEX) and operational costs (OPEX) were estimated using the technical data obtained. Moreover, a sensitivity analysis was performed to understand which elements had a bigger impact on the total costs.

The results obtained are attractive and present the order of magnitude of the investment required for the execution of this proposal to TERSA. In case that this conceptual design considered of potential strategically of interest, the next step required would be the start of the basic engineering phase or pre-FEED.

Acknowledgements

First and foremost, I would like to thank both directors of this Master's Thesis, Prof. José Luis Cortina and Prof. César Valderrama, for their wise advice and support given throughout all stages of this project. I truly appreciate the fact that they didn't just approve the topic of this Thesis but also challenged it, in order to improve it.

I would also like to extend my gratitude towards all the TERSA team involved during this project. I am grateful for having had the opportunity to apply my ideas to a real case scenario, in which the company has been so proactive.

Last but not least, special thanks to my colleagues, friends and family that have given support during all this Master's.

Glossary of terms

AEL Alkaline Electrolysis

AMB (Barcelona Metropolitan Area)

CAPEX Capital Expenditure

CEPCI Chemical Engineering Plant Cost Index

CCS Carbon Capture and Storage

CCU Carbon Capture and Utilization

EOC Environmental Opportunity Cost

EOR Enhanced Oil Recovery

GHG Greenhouse Gases

MSW Municipal Solid Waste

OPEX Operational Expenditures

PEMEL or PEM Proton Exchange Membrane Electrolysis

PtG Power-to-Gas

PtM Power-to-Methane

PV Photovoltaic module

RWGS Reverse Water-Gas Shift reaction

SNG Synthetic Natural Gas

SOEL Solid Oxide Electrolysis

SRC Steam-raising fixed bed reactor

STP Standard conditions for Temperature and Pressure

WGS Water-Gas Shift reaction

Table of contents

1. Introduction

Nowadays, the concern for global climate change among society has grown so much that it drives international and local policymakers. Considerable efforts have been made in the last few years to increase renewable energies in all sectors responsible for greenhouse gases (GHG) emissions. In the global framework, the Paris Agreement was the first-ever universal, legally binding global climate change agreement, adopted in the Paris climate conference (COP21) of 2015. Governments agreed to a long-term goal of keeping the increase in global average temperature well below 2 °C above pre-industrial levels, while aiming to limit it to 1.5 °C by 2100 [1]. In the European framework, GHG emission reduction targets were set by EU leaders in 2007 to reduce the emissions by 20% by 2020. This target was accomplished since GHG emissions were reported to be reduced by 24% between 1990 and 2019. In the long term, the European Green Deal aims to be an economy with net-zero GHG emissions by 2050. In addition, an intermediate milestone of 40% reduction was set to be reached by 2030, which will now be updated with a new proposal of reaching a reduction of at least 55% [2]. Thus, negative emission technologies (NETs) need to be deployed to reach the regulation targets. Example of NETs include direct carbon dioxide air capture, indirect CO_2 capture due to afforestation, algae culture or carbon capture utilization and storage (CCUS). Carbon capture technologies are implemented into industrial systems that emit a significant amount of CO_2 in their flue gases.

Municipal solid waste (MSW) generation is directly related to the population growth and industrial activities. Its generation is expected to increase from nearly 1.3 billion tons per year in 2019 to 4.0 billion tons per year in 2025 [3]. Landfill regulation has become stricter and current EU regulations focus on waste hierarchy (preparing for re-use, recycling, recovery and disposal), being landfilling the least preferable option. The European Landfill Directive limits the share of MSW landfilled to 10% by 2035 [4]. Other action from the European Green Deal point towards favoring a circular economy background by penalizing the practices that do not follow the waste hierarchy. As it is shown in Figure 1 about 45% of waste was landfilled in Spain in 2018. Thus, lots of efforts shall be taken to reach the European targets. One alternative is to follow the waste hierarchy and move one step upwards, from landfilling to energy recovery. Waste-to-energy (WtE) is underdeveloped in Spain with a weight lower that 5% of the total treatment types. Although WtE plants flue gases comply with strict regulations, they are a stationary CO_2 emitter that is reasonably large for the implementation of CCUS [3]. Thereby, the two concepts of landfilling avoidance and CCUS could be combined to achieve negative CO_2 emissions, since a fraction of MSW contains biogenic CO_2.

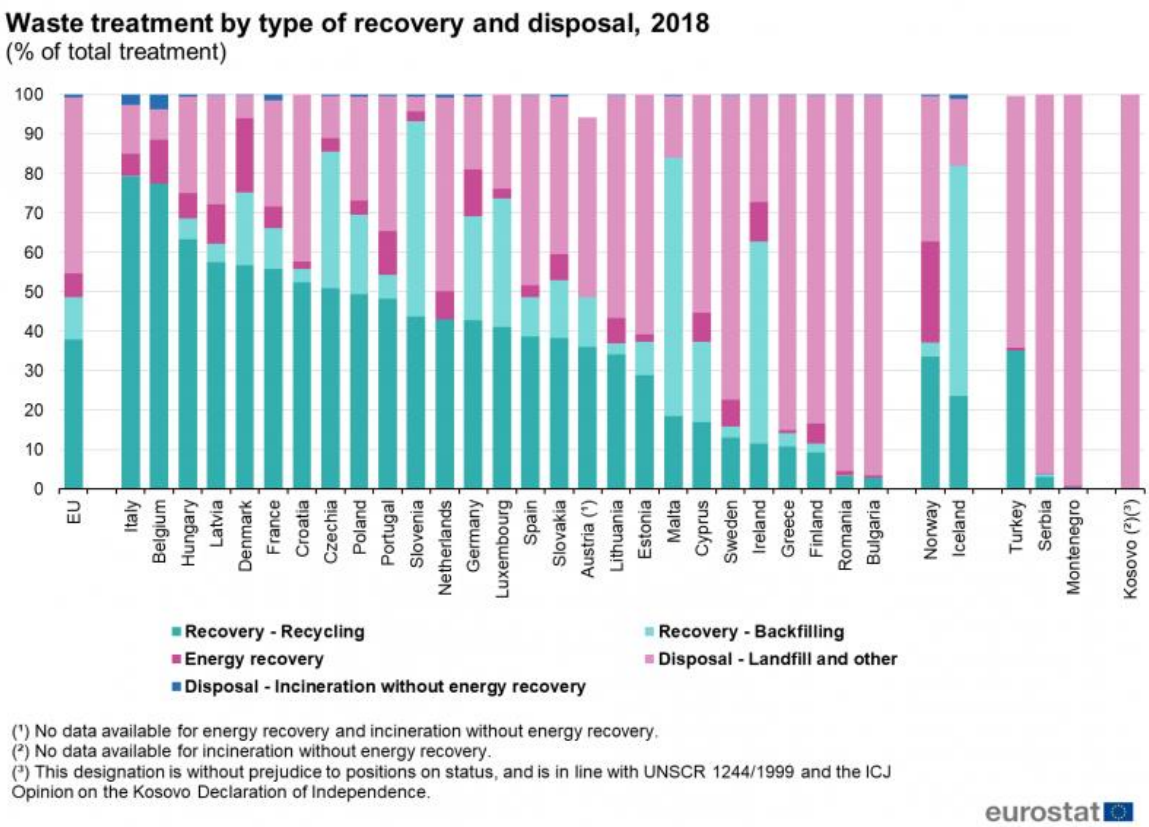

Figure 1. Waste treatment by type of recovery and disposal, 2018 [5]

Carbon capture and utilization (CCU) purpose is to re-use the CO_2 as a feedstock for various applications. CO_2 is seen as an alternative feed which can reduce the demand on natural resources and their traditional exploitation that follows a linear economy scheme. CCU has many applications such as biological conversion, food and drink industry, plastics, refrigerants, chemicals production, mineralization, fire suppression, as an inert agent, among others [6]. CCU constraint is finding the best application for the captured carbon. The ideal application uses the CO_2 as close to the origin source as possible, in order to avoid transportation costs and emissions.

1.1. Description of the plant

The selected WtE plant in this case study is the Sant Adrià de Besòs Municipal Solid Waste Recovery Facility, owned by TERSA. It is a municipal solid waste treatment center for the Barcelona Metropolitan Area (AMB). Two plants operate on the same site using different yet complementary treatment processes [7]:

- Mechanical-Biological Treatment Plant (MBTP). This facility went into operation in 2006. Here materials and energy are recovered from mixed municipal solid waste deposited in grey street bins.
- The Waste-to-Energy (WtE) Plant became operative in 1975. It recovers energy from residues generated at the Mechanical-Biological Treatment Plant and at other metropolitan plants.

  The unrecoverable material from the MBTP is burnt in three furnaces. In the furnace, this material is burnt at 850 °C for approximately 20 min. The hot gases given off are used to heat water to 400 °C in the boiler. The steam is fed through a turbine, the movement of which generates electricity. Then, the steam remains so hot this it is used by the centralized district heating and cooling system. The bottom ash produced in the furnaces are sorted into scrap metal and gravel. While scrap metal is recycled, gravel can be used for road beds and other civil works.

  The gases produced during the process are cleaned. First, urea is injected in the furnace to neutralize NOx. On the outlet of the boiler there is an electro-filter, which extracts the largest particles using magnetism. Then, it is sprayed with quicklime which reacts with the acidic gases. Also, activated carbon is injected, which absorbs dioxins and metals. Finally, the gas is passed through a bag filter which retain the fine particles, lime and activated carbon [7]. The latest upgrade of the WtE in 2021 consisted in the installation of a new catalytic system that reduce the NOx emissions up to 50% [8].

Figure 2. TERSA's waste-to-energy plant in Sant Adrià del Besós [9]

1.2. Objective

The objective of this work is evaluate the carbon recovery and utilization routes at TERSA WtE plant. All proposed scenarios shall follow the carbon capture and utilization, and circular economy schemes. The following points shall be included in the techno-economic assessment:

- A technical viability assessment and sizing of the main process equipment.
- An economic estimate of the capital and operational expenses (CAPEX and OPEX).
- An economic estimate of the expected revenues or savings, in comparison with the current WtE plant operation.
- A sensitivity analysis of the costs.
- A comparison of the total costs of the different scenarios.

The final goal is to provide enough techno-economic information to TERSA, so the company can take a decision in the future about whether or not studying in more detail any alternative proposed in this work.

2. State of the art

This chapter contains the state of the art of the several technologies and processes that have considered in this work for carbon recovery and utilization in waste to energy (WtE). Following the process flow, the starting unit is the capture of the carbon dioxide from the flue gases stream, which leads to its utilization. In addition, a section is dedicated to hydrogen production technologies since it is needed in the utilization pathways of the CO_2.

2.1. Carbon capture

Carbon capture technologies can be differentiated into three main groups: pre-combustion, oxy-fuel and post-combustion technologies.

Pre-combustion capture of CO_2 is one of the major technology options for brand new gasification plants (greenfield projects). Waste is gasified in a low-oxygen atmosphere where it undergoes a partial oxidation to obtain syngas. The reducing atmosphere pf the process limits the emissions of furans and dioxins that often are the consequence of the waste combustion [10]. Gasification products are fed in the water-gas swift reaction to convert them to CO_2 and H_2. While the first one can be separated and furtherly stored or used, the other one can be directly used. The drawback of this type of technology is the need of an air separating unit to feed the furnace with the required oxygen concentration [11].

Oxy-fuel combustion involves the replacement of air as an oxidant into high purity oxygen, usually above 95%(v), and recirculated flue gas. Consequently, produced flue gas stream contains mainly carbon dioxide and water vapor that can be easily removed by condensation [12]. One of the main advantages of oxy-fuel combustion is that the emission of NOx, SO_2 and CO can be reduced successfully [13]–[15]. The concerns of the implementation of this technology are related to the use of low-quality fuels, such as municipal solid waste (MSW), and to the high energy consumption of the air separation unit.

In the present, post-combustion is considered the most mature technology for carbon capture in existing plants [12]. Inside this category, amine scrubbing and membrane capture are the technologies that stand out the most. The first one is currently the most commercially technology and is more widely developed than pre-combustion and oxy-fuel systems [16]. The last one is a promising technology that has some advantages like compactness, modularity, ease of installation by skid-mounting, flexibility in operation and maintenance, and in most cases, lower capital cost as well as lower energy consumption [17]. In addition, it has very little chemicals requirements in comparison to conventional separation

processes [18]. Since membrane technology is the one included in the scope of this project, further details about them are explained below.

2.1.1. Membrane technologies

Gas separation membranes operate on the principle of preferential permeation of the different solutes through its free volume. The main design parameters of membranes are selectivity and permeance. In the case of post-combustion flue-gas, the desirable membrane shall have a high CO_2/N_2 selectivity because N_2 (g) is the most predominant molecule in any WtE flue gas stream. Permeance derives from permeability, the ability of a membrane to permeate gas, and is defined as permeability per membrane thickness [19]. In this process, the gas stream is pressurized and forced to flow through a membrane separator consisting typically into a large number of hollow membranes. Since the membrane has been designed to be selective to CO_2, the permeate stream, is richer in that component. The CO_2 is recovered in the lower pressure on the shell side of the separator [20]. Figure 3 shows the principles of gas separation membranes.

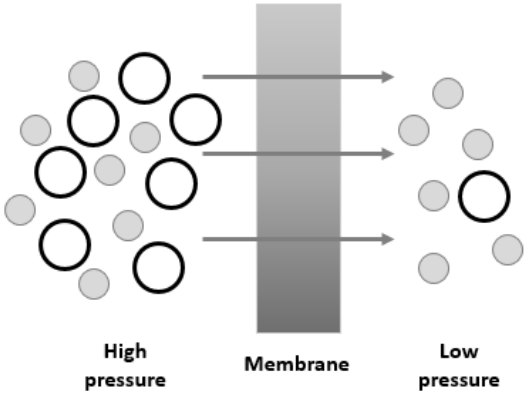

Figure 3. Principle of gas separation membranes [20]

The minimum requirements for membranes to compete against the traditional and more extended monoethanolamine (MEA) absorption process are permeance higher than 500 GPU and selectivity higher than 40 [21]. Currently there are many commercially available membrane types that have been tested in real power plants. PolyActive™ and Polaris™ are made from the most promising materials among those. Table 1 lists the main parameters of these two brands with the addition of the latest Polaris™ generation.

Table 1. Commercially available membrane modules tested with flue gas [21]

Manufacturer	Membrane	Permeance [GPU]	CO_2/N_2 selectivity	Polymer	Reference
MTR	Polaris™ gen 1	1000	50	PE-PA copol.	[22]
MTR	Polaris™ gen 2	2000	49	PE-PA copol.	[22]
Helmholtz-Zentrum	PolyActive™	1480	55	PEO-PBT	[23]

When a higher degree of separation is required than the one obtained with a single stage of membranes, a current cascade of membrane stages can be designed. Ideally, as many stages the process has, the better the separation will be. However, in the case of gas, compression costs are high. Therefore, membrane cascades for gas separation are usually limited to just two or three stages. Depending on the final product specifications, two types of cascades can be chosen. The two-stage stripping cascade is designed to obtain a purer retentate (Figure 4a), whereas a purer permeate is the goal of the two-stage enriching cascade (Figure 4b). It is also possible to design a hybrid cascade by adding a membrane pre-stage to concentrate the desired compound. This may be specially attractive when the feed concentration is low in the component to be passed through the membrane, desired permeate purity is high, separation factor is low, and/or a high recovery of the more permeable component is desired [17].

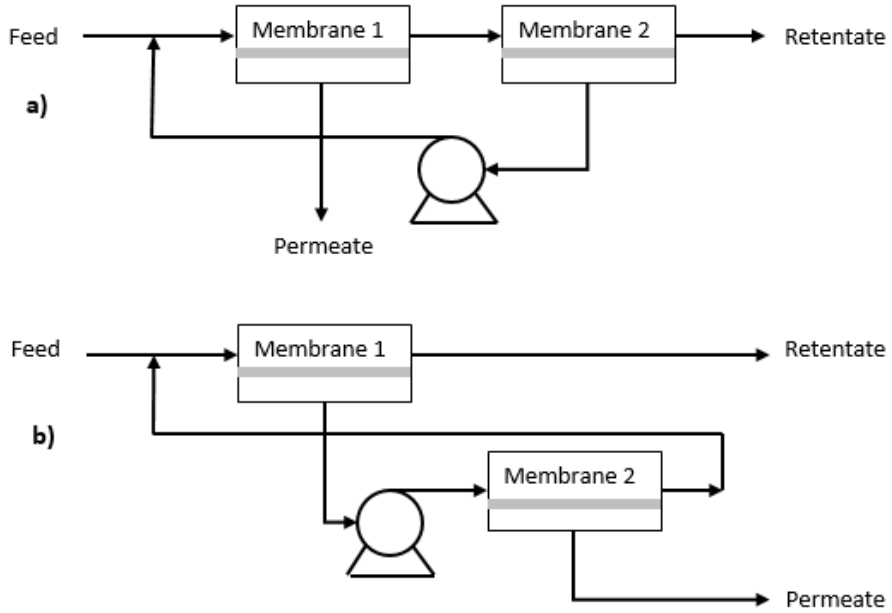

Figure 4. Cascade membrane configuration. a) Two-stage stripping cascade. b) Two-stage enriching cascade [17]

Membrane technologies has the advantage of being a low-cost technology both in terms of CAPEX and OPEX. However, the cost of the plant shall be calculated rigorously. Merkel et al. [24] set an economic analysis of a membrane carbon capture unit in a coal-fired power plant. Since they are the manufacturers of the Polaris™ membranes, similar assumptions may be used in this work. The compressor efficiencies and cost factors collected in Table 2 are average current values for large gas processing systems. The membrane skid cost of 50 USD/m^2 already includes the membrane modules, housings, frame, valves and piping. The two main parts that contribute to the OPEX of the membrane skid are the cost of the power used in the separation process and the interest and depreciation costs. Equation (1) calculates the cost of capture (CC) in USD/ton CO_2 where P is the power required for CO_2 capture equipment (kW), T is the plant capacity factor (h/y), E is the cost of electricity (USD/kW), C is the capital cost of the capture equipment, which is the sum of the costs of compression and skid, (USD), and F_{CO2} is the mass flowrate of captured CO_2 (ton/h).

$$CC = \frac{(P \times T \times E) + (0.2 \times C)}{F_{CO_2} \times T} \quad (1)$$

An additional factor of 20% of the total membrane plant cost is applied, which should be enough to cover depreciation, interest, normal labor and maintenance cost.

Table 2. Assumptions used in base case design calculations by [24]

Category	Value	Units
Compressor efficiency	0.80	-
Compressor cost	500	USD/kW
Membrane skid cost	50	USD/m^2
Membrane equipment installation factor	1.6	-
Capital depreciation/interest	20	%/year
Cost of power	0.04	USD/kW
Capacity factor	85	%
Power plant lifetime	25	Years

2.2. Carbon dioxide utilization

Two main pathways for the carbon, after being captured, have been explored in the last decades: i) Carbon Capture and Storage (CCS) and ii) Carbon Capture and Utilization (CCU), being its main difference in downstream processes after CO_2 capture. As their name indicate, while CCS aim is to store the carbon underground for a long term, CCU seeks to reintroduce the carbon (stored) into its economic cycle by refurbishing and transforming it to new raw materials following the circular economy approach.

Currently, one of the main applications for CCS is Enhanced Oil Recovery (EOR). EOR focuses on the injection and sequestration of CO_2 in underground depleted oil reservoirs [25]. Although this technology has been proved feasible, it depends on the availability of sites to store the carbon for a long period of time. Since, the CO_2 is produced (and thus captured) all around the world and sequestered only in certain known areas, CCS presents a big logistic issue in the areas where the storage cannot be guaranteed. Also, the main point of storing the carbon is to reduce its atmospheric emissions. So, if more than one molecule of CO_2 is emitted per molecule stored, the whole process does not solve the initial problem.

CCU looks like the solution that fits best the circular economic paradigm by converting the CO_2 into products for the chemical industry. Renewable energy connects the different industrial sectors to a cross-industrial network. Thereby fossil fuels in one industry are replaced by the carbon rich gases that are emitted as a carbon source [26]. By recapturing the carbon to use it as a C1 building block, the carbon is supplied to a circular value chain. To assure that CCU reduces the carbon emissions, the whole process of capture, re-conditioning and supply has to be fed with renewable energy sources that do not add carbon to the already fragile cycle.

2.2.1. Power to methane

Power-to-methane process (PtM) has three main process stages: i) water electrolyzer, ii) CO_2 separation unit and iii) methanation unit. H_2 is generated by water splitting in the electrolyzer. Then, the captured CO_2 and the produced H_2 are mainly converted to CH_4 and H_2O. The product is treated to enrich the CH_4 composition. Finally, synthetic natural gas (SNG) or bio-methane is produced. This SNG can be used as fuel for mobility, in the residential sector, for power generation and as raw material for the industry [27].

In the case that SNG is desired to be injected into the current natural gas grid, it must be compressed to sufficient pressure. If it is injected in the transmission grid, it shall be compressed typically 40 to 60 bars. Whereas the distribution grid only requires between 5 to 10 bar [28]. Quality requirements of

biogas injection to the Spanish grid are published in BOE-A-2018-14557 [29]. Gases produced from non-conventional sources, such as biogas obtained from biomass or microbial digestion, have lower methane purity requirements. Table 3 lists the threshold requirements for non-conventional biogas in Spain. Bio-methane produced from CO_2 from WtE flue gases and green hydrogen is included inside this special category. As a general rule, the minimum methane concentration for ordinary methane is 96% vol. as minimum [30]. Natural gas and bio-methane are currently being injected into European grids, so this is a market that has already been tested.

Table 3. Biogas threshold values for injection into the Spanish distribution grid [29]

Component	**Threshold value**	**Component**	**Threshold value**
CH_4	>90% vol.	F	10 mg/m^3
H_2	<5% vol.	Cl	1 mg/m^3
CO_2	<2% vol.	NH_3	3 mg/m^3
CO	<2% vol.	Hg	1 µg/m^3
O_2	<1% vol.	Siloxanes	10 µg/m^3
H_2O	Dew point < -8 °C	BTX	500 mg/m^3

The overview of the power-to-gas (PtG) concept is shown in Figure 5, where PtG is applied in a WtE facility. The existing parts of the plant are in black and the new units to be added are in blue. The final products are circled in blue as well (energy, CH_4, H_2 and O_2). According to Figure 5, renewable electricity is used to feed the electrolyzer, which produces pure O_2 and H_2. The first one can be either released to the atmosphere or, preferably, sold to other industries or as a final sub-product. The later one is the first main product of the PtG plant. It can be transferred to electric power, as fuel in the mobility sector, or as industry feedstock. In the last case, the chemical, petrochemical and metallurgical industries currently produce H_2 by methane steam reforming, which is not as clean as electrolysis. The second process step is methanation, which is fed with the captured CO_2 gas from the exhaust gases of the WtE plant. The main advantage of methane as a product is that its supply chain is existing and well-stablished. SNG bi-directionally links the power grid and the gas grid [31].

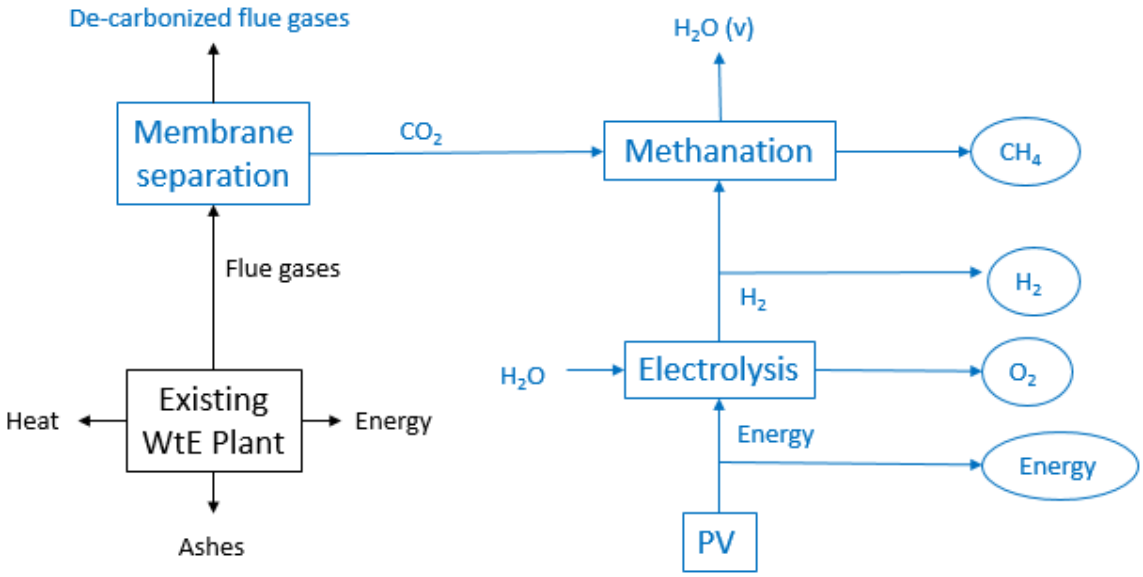

Figure 5. Power-to-Gas concept in a WtE plant

Any technical process that uses electricity to produce an energy vector need to have minimum energy and exergy losses. According to Sterner et al. (Table 4) [32], H_2 conversion performs better than SNG since the last one uses the first conversion as its starting point. The efficiency of the conversion is around 70-85% of chemical methanation and is added to the electricity to H_2 step [31]. However, as mentioned beforehand, the methane grid is already stable and in use. SNG could be an intermediate solution before the economy shift towards the hydrogen-based scheme.

Table 4. Efficiencies for PtG electricity to gas process chains [32]

Path	Efficiency (%)	Boundary conditions
Electricity → H_2	57-73	Including compression to 80 bar (feed in gas grid for transportation)
Electricity → SNG	50-64	
Electricity → H_2	64-77	Without compression
Electricity → SNG	51-65	

The reaction of the chemical methanation of CO_2, also called Sabatier reaction, is a reversible high exothermic reaction described in Equation (2) [30]:

$$4\,H_2(g) + CO_2(g) \leftrightarrows CH_4(g) + 2\,H_2O\,(l) \qquad \Delta H_{298K} = -165\ kJ/mol \tag{2}$$

The methanation reaction takes place through two reaction mechanisms: in the first one, the reverse water-gas shift reaction converts carbon dioxide into carbon monoxide and water (*3*). Then, it is followed by carbon monoxide methanation (*4*).

$$CO_2(g) + H_2(g) \leftrightarrows CO(g) + H_2O\ (l) \qquad \Delta H_{298K} = 41\ kJ/mol \tag{3}$$

$$CO(g) + 3\ H_2(g) \leftrightarrows CH_4(g) + H_2O\ (l) \qquad \Delta H_{298K} = -206\ kJ/mol \tag{4}$$

The global reaction is exothermic and the moles difference is negative, therefore the synthesis is thermodynamically favored toward products at low temperature (around 280°C) and high pressure (around 5 bar). The state of the art catalyst is based on nickel because its high activity and low price [27], [30].

Heat management is key in reactor design because the methanation reaction is highly exothermic. Since this process is widely applied, various reactor types have been adapted for this process. The most relevant ones are fixed-bed, monolith, microchannel, membrane and sorption-enhances reactors [27].

- **Fixed-bed reactors** are the most used ones for this application. Commonly, a cascade of adiabatic reactors in series is installed separated. They are separated by heat exchangers that cool the process gas to the desired inlet temperature in order to obtain high CO_2 conversions. In the reactors, the catalysts are packed in static beds where the gas is passed through. The adiabatic reactors are relatively simple and cost-effective systems. On the other hand, the polytropic design is a cooled tube-bundle system. In this type of fixed-bed reactor, lots of tubes of relatively small diameter are placed in parallel. In comparison to adiabatic reactors, polytropic reactors exhibit lower temperature gradients that lead to a longer lifespan of the system. However, these reactors are more expensive and relatively complex. Fixed-bed reactors are offered on the market, e.g., from Outotec, Etogas and MAN.
- **Monolith reactors** have the advantage of having a high specific catalyst area, small pressure drop and small response time. They have been widely used in exhaust gas cleaning in the automobile industry. However, their main disadvantage is the difficulty of installation at the large industrial scale.
- **Microchannel reactors** have the inherent advantage of process intensification. Hydrodynamics and heat transfer are improved due to the small size of the channels. Their main concern is catalyst deactivation because the whole reactor has to be replaced since the catalyst is fixed on the inner surface of the reactor.
- **Membrane reactors** combine the chemical reaction with membrane separation, to increase the CO_2 conversion. Due to Le Chatelier's principle, the removal of H_2O (product) shifts the equilibrium of the methanation reaction towards the products, so more CO_2 is produced. The

main disadvantage of these reactors is that membranes need replacement at regular intervals and that would suppose a big impact in the costs.

- The **sorption-enhanced reactor** concept is also based on Le Chatelier's principle. The conversion is increased up to almost 100% by using a mixture of an adsorbent and a catalyst in the reactor. Similar to membrane reactors, the adsorbent is the one that removes some of the products and shifts the equilibrium to the right side of the reaction. Although the conversion is very high, this technology could have short life-time due to the adsorbent regeneration cycles.

Currently there are few plants worldwide that produce green energy and use it to produce CH_4 from captured CO_2. Three plants are used as an example to show that PtM is a commercially available process. Their main parameters are summarized in Table 5 [33] and furtherly explained bellow.

Table 5. Industrial-scale PtM plants [33]

Plant	Methanation technology	Capacity
ZSW demonstration plant	Tube-bundle reactor (alone or with a plate reactor)	250 kW_e
Audi e-gas plant	Isothermal fixed bed	325 Nm^3 SNG/h
HELMETH project	Two fixed-bed reactors in series	5.4 Nm^3 SNG/h

- ZSW power-to-gas- 250 kW_e was developed in 2012 and was the largest PtG plant of this type at that time. The main objective of it was to test different fixed-bed reactor technologies for methanation, mainly plate versus tubular rectors. The system was composed by two fixed-bed reactors, with a capacity for 50 l of catalyst. The first one was refrigerated by water, while the second one by molten salt. After a condensation stage between reactors and a recirculation of the final gas towards the first methanator, the methane content achieved was 99%. The purity was achieved thanks to processing the gas with membrane technology after methanation [33].
- The Audi e-gas plant, built in 2013, is the largest power-to-SNG facility in the world (6 MW_e). It contains a single isothermal fixed-bed reactor where the catalytic methanation of pure hydrogen and carbon dioxide takes place. The hydrogen is produced in 3x2.0 MW_e alkaline electrolyzers powered by an offshore wind park in the North Sea. The CO_2 is captured from raw biogas of a neighboring bio-methane plant by means of amine scrubbing. The Audi e-gas plant has 54% efficiency and produces SNG with 13.85 kWh/kg of energy content [33].

- HELMETH project was launched in 2014 with the aim the demonstrate efficiencies above 85% in PtG systems by integrating high temperature electrolysis (SOEL) and CO_2 methanation. The small-scale 15 kW_e SOEL worked at 800 °C and 15 bar. Methanation process was split in two reactors in series operating at 300 °C and 30 bar, with intermediate water removal [33].

Not much literature is available about methanation investment costs. Outotec GmbH [34] reported investment costs (CAPEX) of 400 EUR/kW SNG for a 5 MW plant and 130 EUR/kW SNG for a 110 MW plant (both data sets are for 2014 and 20 bar operating pressure) [35]. An approximate estimate of the capital cost can be obtained from a knowledge of the cost of earlier projects using the same manufacturing process [36]. The capital cost of a project is related to capacity by Equation (5)

$$C_2 = C_1 \left(\frac{S_2}{S_1}\right)^n \tag{5}$$

where C_2 = capital cost of the project with capacity S_2; and C_1 = capital cost of the project with capacity S_1.

The value of the index *n* is traditionally taken as 0.6, known as the six-tenths rule. If the data from Outotec is applied in (5), the resulting *n* is 0.62, which is very close to the heuristic from Sinnot [36]. An alternative cost function is shown in Equation (6) [37]. The cost for Sabatier reactors is extrapolated from literature data. A cost of 8000 EUR/kg for small reactors is assumed to be conservative considering a coefficient of 0.7 to take into proper account the influence of the size.

$$C_{CAPEX,Sabatier} = \left(8000 \cdot M_{produced}\right)^{0.7} \tag{6}$$

Other cost estimate studies have been made for chemical methanation processes where each equipment is designed and, afterwards, the component cost method is applied [38]. This approach leads to more accurate estimations because the calculation fits the exact process. On the other hand, it requires a full design of the plant and usually the data needed to develop the study is scarce.

2.2.2. Power to methanol

Methanol (MeOH) is the simplest, safest, and easiest way to store and transport liquid oxygenated hydrocarbons. Currently, is mainly produced from syngas obtained from incomplete combustion and from the reforming of fossil fuels, mainly natural gas or coal. Replacing the feed from syngas with recycled CO_2 and green hydrogen would help to mitigate the major human activity cause of climate change due to excessive burning of fossil fuels.

Besides from its use for energy storage and fuel, methanol serves as raw material for basic chemicals such as formaldehyde, acetic acid and a wide variety of other products, including polymers, paints,

adhesives, construction materials, synthetic chemicals and pharmaceuticals. Moreover, MeOH can be converted into ethylene or propylene via the methanol-to-olefin process (MTO). Practically all hydrocarbon fuels and products currently obtained from fossil fuels could be obtained from methanol instead [39]. Therefore, methanol is a possible CCU pathway that reintroduces the CO_2 in the economy loop via quality products. Figure 5 can be transposed to the power-to-methanol scheme by changing the methanation block to the following process step.

Methanol formation proceeds predominantly via CO_2 hydrogenation according to reaction (7):

$$CO_2(g) + 3\,H_2(g) \leftrightarrows CH_3OH + H_2O \qquad \Delta H = -49.4\ kJ/mol \tag{7}$$

The reaction pathway is furtherly detailed in reactions (8) and (9):

$$CO_2(g) + H_2(g) \leftrightarrows CO(g) + H_2O \qquad \Delta H = 41.2\ kJ/mol \tag{8}$$

$$CO(g) + 2\,H_2(g) \leftrightarrows CH_3OH \qquad \Delta H = -90.6\ kJ/mol \tag{9}$$

The global reaction is exothermic and involves a decrease of volume. The optimal feed gas ratio has been proven to be 3 to 1 H_2/CO_2. Nowadays, all commercial catalysts are based on CuO and ZnO in most cases on a carrier of Al_2O_3. In industrial applications the common catalyst life time is 4 to 6 years. Life time is limited by catalyst deactivation caused by poisoning and thermal sintering. Major poisons for copper catalysts are sulfurs in the range of 0.05-0.5 ppm_v and chlorides over 1 ppb_v [40].

Current reactor designs are dominated by quasi-isothermal steam-raising fixed bed reactors (SRC). SRC were introduced for the first time by Lurgi, now inside the Air Liquide matrix, in the 1970s. Lurgi's design is based on a tubular reactor. The feed gas flows in an axial direction through the tubes, which are filled with the catalyst. The gas is cooled down by the surrounding boiling water on the shell-side. About 80% of the reaction heat is converted to medium pressure steam. Operating parameters for CO_2 conversion are in the range of conventional syngas processes (T ≈ 250 °C, P ≈ 50-100 bar, GHSV ≈ 10000 h^{-1}), GHSV being the gas hourly space velocity (the ratio of feed gas volume at STP to catalyst volume). In general, after the methanol synthesis, the products are passed through a distillation tower to separate MeOH from water and other residual gases. Several pilot plants, that developed the idea of using CO_2 as raw material instead of CO/H_2 syngas, have been built in the recent years [40].

- The development of the first proposal in the 1970s by **Lurgi** led to a single-stage CO_2 to methanol pilot plant presented in **2011** that showed a total CO_2 conversion of 94-97% (per pass conversion of 30-45%).
- The **CAMERE process** (carbon dioxide hydrogenation to form methanol via a reverse water-gas shift reaction) is a two-stage concept developed by the Korean Institute of Science and Technology (KIST). The fist reactor focuses on the endothermic RWGS reaction. It is electrically

heated and operated at 600-700°C with a CO_2 to CO conversion of 60%. Due to the increase of CO content and removal of by-product water, the second methanol synthesis reaction yield is increased and recycle gas ratio is reduced. A 75 kg per day pilot plant has been constructed in combination with a pilot plant for CO_2 separation from a power plant, reaching a MeOH yield of 70%.

- **Carbon Recycling International (CRI)** commissioned the first carbon dioxide to methanol industrial-scale plant in 2012 with a capacity of 13000 t MeOH per year. The plant located in Iceland recycles 5600 t per annum of CO_2 released by a nearby geothermal power plant. The produced MeOH received certification for a 90% reduction of CO_2 emissions compared to fossil fuels according the EU Renewable Energy Directive. The specific emissions were determined to be 0.17 t_{CO2}/t_{MeOH}
- Within the EU Horizon 2020 project **MefCO2**, a demonstration plant was set up in 2019 capturing 500 t per year of CO_2 from a coal power plant in Niederaussem (Germany). The production volume achieved was 400 t per year of MeOH.

The general outcome of the new power-to-methanol plants is that based on the stoichiometry of methanol formation from CO_2, 1.37 t_{CO2}/t_{MeOH} are utilized. Assuming an overall carbon conversion of 96%, this results in a CO_2 demand of 1.43 t_{CO2}/t_{MeOH} [40].

Methanol reactor capital costs (C) can be estimated from literature values of commercial large-scale plants. The cost function in terms of the mass flowrate (M_{in}) (in ton/h) of the gas entering the reactor is Equation (10). A standard factor of 0.65 is employed in order to consider the size effect on investment costs [41], [42].

$$C = 14.2 \cdot 10^6 \cdot \left(\frac{M_{in}}{54000}\right)^{0.65} \quad (10)$$

Concerning the environmental impact of the power-to-methanol scheme with recycling of CO_2, it has been proven that when 1 ton of CCU methanol offsets 1 ton of conventional methanol, the net CO2 emitted is -160 kg. The negative value indicates that every ton of CCU methanol avoids the emission of 160 kg of CO_2 to the atmosphere. However, if the environmental opportunity cost (EOC) is taken into consideration the overall result can change. The potential CO_2 emissions that can be avoided by offsetting CO2-intesive fossil-fuel electricity on the grid is called EOC. In this case, it is the cost of using renewable energy (RE) to produce methanol, instead of injecting it to the grid to replace fossil-fuel based electricity. Thus, the EOC is variable as it depends on the CO_2 intensity of the electricity grid. The same PtX plant that is environmentally favorable in one country can be the opposite in another place. It has been foreseen that unless the CO_2 intensity of the grid mix is lower than 67 g CO_2/kWh, utilizing RE on the electricity grid will produce a greater CO_2 benefit than in CCU methanol production [43].

2.2.3. Carbon dioxide mineralization

At the end of 2014 a new process was commissioned at line 3 of the Twence WtE plant located in Hengelo, the Netherlands. In this process, the CO_2, which had been vented to the atmosphere was scrubbed from the flue gas and used to produce sodium bicarbonate slurry. The new plant started to produce 8000 tons of sodium bicarbonate slurry annually and 2000 tons per year CO_2 was captured from flue gases to produce it. The main advantage of this process change was that the raw material of this bicarbonate changed to sodium carbonate, which was cheaper. Besides having a negative carbon impact, another advantage was that 1 ton carbonate was converted to 1.6 ton bicarbonate. This resulted in additional savings due to lower transportation costs [44].

The sodium bicarbonate slurry produced contained 35% of solid $NaHCO_3$ and was synthesized according to the following chemical reaction (11) [45]:

$$Na_2CO_3(aq) + H_2O(l) + CO_2(g) \rightarrow 2\ NaHCO_3(aq) \qquad \Delta H_{298K} = -42.99\ kJ/mol \tag{11}$$

To sum up, the process was designed to obtain a high carbonate conversion (>90%) and almost 100% conversion of CO_2. It can be summed up as [44]:

$$Na_2CO_3(30\ wt.\%\ solution) + CO_2(pure\ gas) \rightarrow NaHCO_3(35\ wt.\%\ solids) \tag{12}$$

The Twence business case had a payback period of the new process estimated around five years [44]. So, it was proven that this process was economically viable.

Currently, TERSA uses quicklime (CaO) slurry instead of bicarbonate to neutralize the acid gases. Although quicklime is cheaper than bicarbonate, it is a viscous slurry that causes lots of maintenance problems in their pipes. That is the reason why TERSA plans on changing to a solid reagent like sodium bicarbonate in the near future. Therefore, producing the bicarbonate in-house, like at Twence, is seen as an opportunity for TERSA to move into the circular economy approach.

Sodium can be produced from three different main processes: soda ash carbonation from trona mineral, the Solvay process and the sodium sulfate route [46]:

- **Trona** is a natural mineral which contains mainly a mixture of carbonates. This mineral is relatively abundant and widely distributed around the planet, found in places like Namibia, Turkey, Tanzania, China and Wyoming (USA). For the last location, over 20 million tons of trona are mined annually in the Green River Basin. Removal of sodium carbonate from trona is given by heating at temperature of approximately 200 °C. The decomposition of the mineral generates Na_2CO_3, CO_2 and H_2O as seen in Equation (13). Finally baking soda is produced in the carbonation reaction, Equation (7), at 57 °C.

$$2\ (Na_2CO_3 \cdot NaHCO_3 \cdot 2\ H_2O) \rightarrow 3\ Na_2CO_3 + \ CO_2(g) + 5\ H_2O \quad (13)$$

- The **Solvay process** starts with an aqueous solution of sodium chloride, in which ammonia is dissolved and carbonation is carried out with carbon dioxide injection. The main reaction, Equation (14), is promoted as a double exchange reaction, where the sodium ions are carbonated and the chloride anions attach the ammoniac cations. Afterwards, the sodium carbonate can be precipitated and filtrated, or heated up to form soda ash. If soda ash is obtained, it can be transformed to baking soda through the same process described in the previous point.

$$2\ NH_4HCO_3(aq) + 2\ Na^+(aq) + 2\ Cl^-(aq) \rightarrow 2\ NaHCO_3(aq) + 2\ NH_4Cl\ (aq) \quad (14)$$

  Significant amounts of ammonium chloride are produced as a side product. However, it can be removed by simply heating the salt between 40 and 60 °C, and the aqueous solution can be mixed with calcium hydroxide and heated to recover the ammonia.

- **Sodium sulfate** is an alternative to the main two processes explained above. The mechanism of this sodium bicarbonate production route begins with the dissolution of the salt in the solvent, followed by gasification of the main reactants (ammonia and carbon dioxide). The global reaction is a double exchange of sulfate and ammonia ions (15).

$$Na_2SO_4 + 2\ NH_3 + 2\ H_2O + 2\ \ CO_2 \rightarrow (NH_4)_2SO_4 + 2\ NaHCO_3 \quad (15)$$

  The main drawback of this process is that the main reaction may lead to the formation of double sodium and ammonium sulfates, which is a salt of difficult separation.

2.3. Hydrogen production

Both Power-to-Liquid and Power-to-Gas CCU strategies need hydrogen as a raw material. However, this hydrogen must not have a relative positive environmental impact in its supply chain. Hydrogen can be classified according to its environmental impact [47].

- **Grey hydrogen** is produced from fossil fuels and CO_2 is emitted to the atmosphere during the process, such as in the steam reforming of natural gas. In addition, the concept of black hydrogen can be used when the source of H_2 is coal and brown hydrogen when it is lignite. Grey hydrogen is the most consumed type of H_2 in Europe. Around 95% of the produced H_2 does not include any carbon capture step. The emissions allocated to grey hydrogen are 10-11 kg CO_2 / kg H_2.

- **Blue hydrogen** captures the major fraction of the carbon dioxide emissions during its production process. If it is desired to be cataloged as blue, the carbon shall be fixed at least for 100 years after capture. It is defined as hydrogen generated from non-renewable sources that emits less than 4.37 kg CO_2 / kg H_2. The most used technology in this category is steam reforming of natural gas with CO_2 capture.
- **Green hydrogen** is obtained from renewable sources and the environmental impact of the production process has to be low. In terms of emissions, the threshold is set at 4.37 kg CO_2 / kg H_2, the same as blue hydrogen. The concept "green hydrogen" was originated specifically for the production of hydrogen via water electrolysis with RE, making clear the contrast between this and the traditional fossil-fuel-consuming process, now referred as grey hydrogen. Nowadays, the main electrolyzer technologies are AEL (alkaline electrolysis), PEMEL (proton exchange membrane electrolysis) and SOEL (solid oxide electrolysis).

The main layout, specific cathode and anode reactions and properties of AEL, PEMEL and SOEL are discussed in the following.

2.3.1. Alkaline electrolysis (AEL)

Alkaline electrolysis is a mature technology, which has been applied for large-scale hydrogen production in the MW-scale since the beginning of the 20th century. Its traditional basic layout is shown in Figure 6. The electrodes are immersed in a liquid electrolyte separated by a diaphragm. Usually, the electrolyte is a 25-30% aqueous KOH solution. It is circulated to remove the product gas bubbles and heat. The electrolyte is stored in two separate drums for hydrogen and oxygen respectively. The product gas quality after drying is typically in the range of 95.5-99.9% for H_2 and 99-99.8 for O_2. The partial reaction at the electrodes is described by Equation (16) and Equation (17) [48]:

$$2\,H_2O + 2\,e^- \rightarrow\ H_2(g) + 2\,OH^- \qquad Cathode \tag{16}$$

$$2\,OH^- \rightarrow \frac{1}{2}O_2(g) + H_2O +\ 2\,e^- \qquad Anode \tag{17}$$

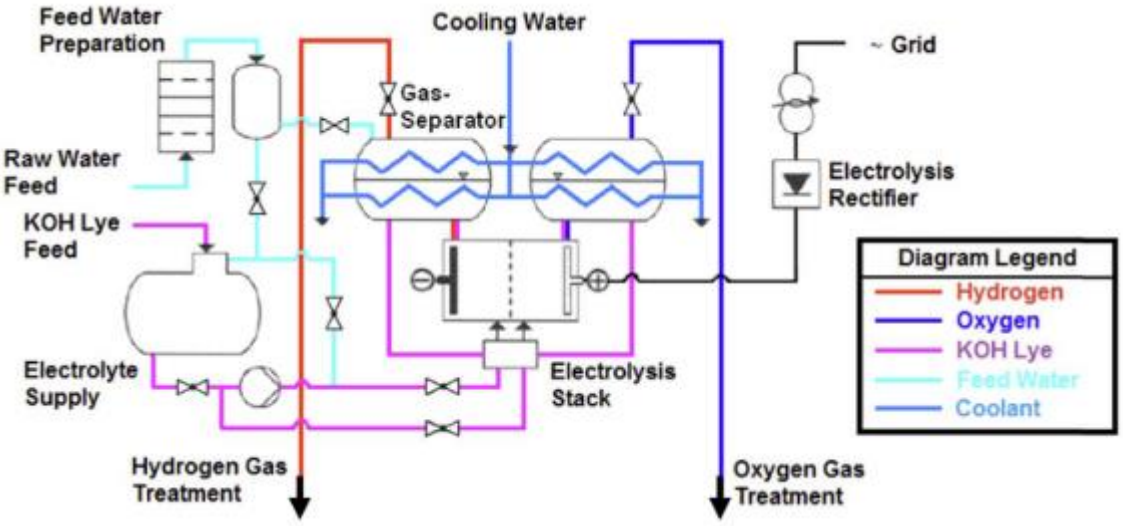

Figure 6. Layout of an alkaline electrolysis system [48]

2.3.2. Proton Exchange Membrane electrolysis (PEM)

Polymer Exchange Membrane (PEM) electrolysis was introduced by General Electrics in the 1960s. The basic layout of a PEMEL is shown in Figure 7. A proton exchange membrane, usually made from Nafion®, separates the two half-cells, and the electrodes are directly mounted on the membrane. Water is supplied at the anode and the following partial reactions take place (18) and (19):

$$2\,H^+ + 2\,e^- \rightarrow H_2\,(g) \qquad Cathode \tag{18}$$

$$H_2O \rightarrow \frac{1}{2}O_2(g) + 2\,H^+ + 2\,e^- \qquad Anode \tag{19}$$

Due to its low cross-permeation, produced hydrogen purity is higher than AEL and around 99.99% after drying. PEMEL features a compact module design because of the solid electrolyte and high current density operation, compared to AEL [48].

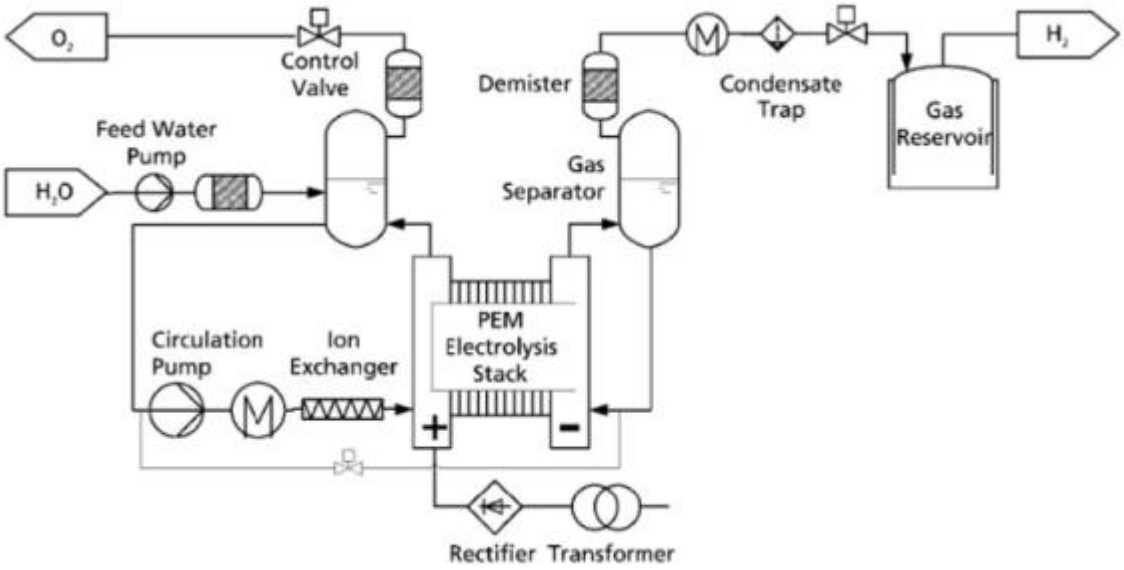

Figure 7. Layout of a PEM electrolysis system [48]

2.3.3. Solid Oxide electrolysis (SOEL)

The development of SOEL begun in the USA in the 1970s by General Electric and Bookhaven National Laboratory, followed by Dornier in Germany. SOEL operates at temperatures of 700-900 °C. High temperature operation results in higher efficiencies than AEL or PEMEL but implies a challenge for material stability. The increase of efficiency results from the fact that kinetics and thermodynamics improve with the operation temperature. A simplified process layout of a SOEL system is given in Figure 8. The reactions at the electrodes are described according to (20) and (21):

$$H_2O + 2\,e^- \rightarrow H_2(g) + O^{2-} \qquad Cathode \tag{20}$$

$$O^{2-} \rightarrow \frac{1}{2}O_2(g) + 2\,e^- \qquad Anode \tag{21}$$

The feed water or steam is pre-heated in a recuperator against the hot product streams that leave the stack. In addition, low temperature heat has to be integrated or electrical heating is required to account for the heat of evaporation. The stack consists typically of planar cells electrically connected in series. Steam, and recycled hydrogen are supplied to the cathode, to maintain reducing conditions, and partly converted to hydrogen. The mixture of steam and hydrogen is separated by cooling and condensing the water. Due to exergetic losses of the heat exchanger and the difference in heat capacity of the make-up steam and the SOEL product gas, the steam has to be further superheated to reach the SOEL inlet temperature of 700-1000°C. The high temperature heat is either supplied by an external heat source or by an electrical heater [48].

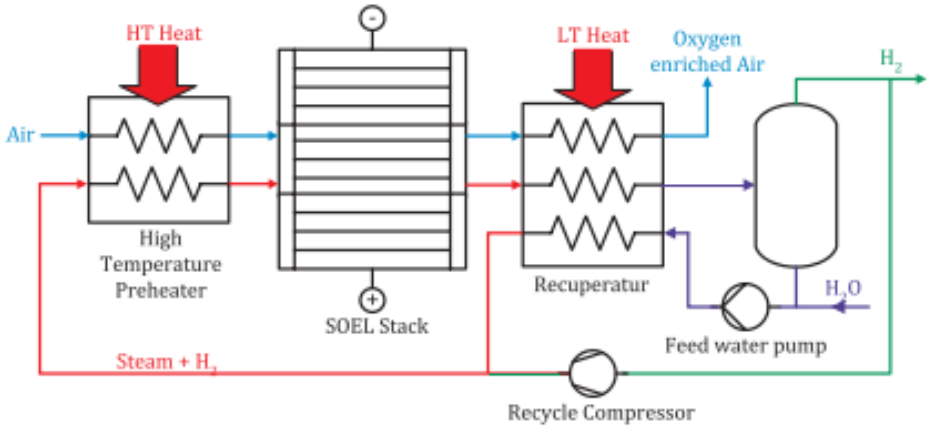

Figure 8. Layout of a SOEL system [48]

2.3.4. Electrolyzer technology comparison

Table 6 summarizes the main parameters of AEL, PEMEL and SOEL. In conclusion, AEL is the most mature technology and it has the lowest specific investment and maintenance costs. It stands out in the large-scale applications. In contrast, PEMEL development has been driven by flexible energy storage application in recent years. PEMEL offers several advantages compared to AEL with regard to compact design, flexibility and shorter start-up times. On the other hand, SOEL is still at pre-commercial stage even though the company Sunfire is offering the first pilot plants [48].

Table 6. Summary of KPIs of state-of-the-art of water electrolysis technologies [48]

	AEL	**PEMEL**	**SOEL**
Operation parameters			
Cell temperature (°C)	60-90	50-80	700-900
Typical pressure (bar)	10-30	20-50	1-15
Current density (A/cm^2)	0.25-0.45	1.0-2.0	0.3-1.0
Flexibility			
Load flexibility (% nominal load)	20-100	0-100	-100/+100
Cold start-up time	1-2 h	5-10 min	hours
Warm start-up time	1-5 min	< 10 s	15 min
Efficiency			
Nominal stack efficiency (LHV)	63-71%	60-68%	100%
…specific energy consumption (kWh/Nm^3)	4.2-4.8	4.4-5.0	3
Nominal system efficiency (LHV)	51-60%	46-60%	76-81%
…specific energy consumption (kWh/Nm^3)	5.0-5.9	5.0-6.5	3.7-3.9
Available capacity			

Max. nominal power per stack (MW)	6	2	< 0.01
H_2 production per stack (Nm^3/h)	1400	400	< 10
Cell area (m^2)	< 3.6	< 0.13	< 0.06
Durability			
Life time (kh)	55-120	60-100	8-20
Efficiency degradation (%/a)	0.25-1.5	0.5-2.5	3-50
Economic parameter			
CAPEX (EUR/kW)	800-1500	1400-2100	> 2000
OPEX (% of annualized CAPEX)	2-3	3-5	n.a.

PEMEL is expected to pair costs with AEL by 2030 and become the preferred technology for electrolysis coupled to renewable generators [49].

3. The TERSA case study

TERSA is a public company that depends on the Barcelona city hall and the AMB being its objective to recover and valorize MSW as efficiently as possible. They treat the unsorted fraction of waste that cannot be recovered after the Mechanical-Biological Treatment Plant, as explained in the Introduction section. TERSA emits through the stack 261440 Nm^3/h of flue gases that mainly contain nitrogen, steam, carbon dioxide and oxygen. The composition was provided directly by TERSA and is summarized in Table1A1 in the Annex section.

An introduction of the objectives of this work was presented to TERSA. Some examples of similar plants that capture the carbon from their flue gases to either using or selling it as a by-product were explained to demonstrate that this CCU route is already viable. After having discussed the general points of CCU, five different process alternatives were presented. The previous state of the art chapter contains all the basic information regarding the processes proposed. Table 7 summarizes the five routes that were presented. All of them had the separation of CO_2 with membrane technology in common. Then, the captured carbon was expected to either be directly used as it is, transformed to bio-methane, or to bio-methanol.

Table 7. Initial process scenarios proposed to TERSA

Scenario #	Carbon Capture	Carbon utilization	Products
A	Remove CO_2	-	-
B	Purify CO_2	Direct use	CO_2
C	Purify CO_2	H_2O electrolysis	CO_2, H_2, O_2
D	Purify CO_2	Power-to-Methane	H_2, O_2, CH_4
E	Purify CO_2	Power-to-Methanol	H_2, O_2, MeOH
F	Purify CO_2	Mineralization	$NaHCO_3$

As a consequence of being a public company, TERSA proposed two main scenarios in which the objective was not to place new products into the market, but to reuse the captured CO_2-based products within the same WtE plant.

It was agreed that membranes were the selected technology to capture the CO_2 from the flue gases. This technology fits this case study because there is a lack of space in the existing plant, mainly because of its geographic localization. The current layout cannot be furtherly expanded because it already limits with coast line regulations and is next to a cogeneration plant owned by another company. Two process scenarios were suggested by TERSA to be studied in detail:

- The bio-methane production route was found interesting because methane is injected to the industrial furnace intermittently to keep the incineration temperature at its optimum. Temperature is key to control the formation of toxic substances such as furans and dioxins.
- The other alternative was based from the WtE plant in the Netherlands. Twence plant produces sodium bicarbonate slurry from their post-combustion captured CO_2. The produced slurry is re-used in the gas cleaning step of the plant. Bicarbonate efficiently neutralizes the acid gases that exit the furnace such as SO_2, SO_3 and HF, among others. At Twence, the excess of bicarbonate production is sold to third-parties.

However, since TERSA's business goal does not include the possibility of selling products, the final solution would capture carbon to exclusively produce the necessary sodium bicarbonate and methane that meets the existing process needs. Both scenarios selected by TERSA, the production of bicarbonate and bio-methane, are going to be explained in more detail in following sections. A preliminary diagram of the methanation and bicarbonate process routes that were found interesting by TERSA is plotted in Figure 9. The parts in black are already existing in the current facility in TERSA, while the blue ones are new product lines and the red ones are new energy consumers.

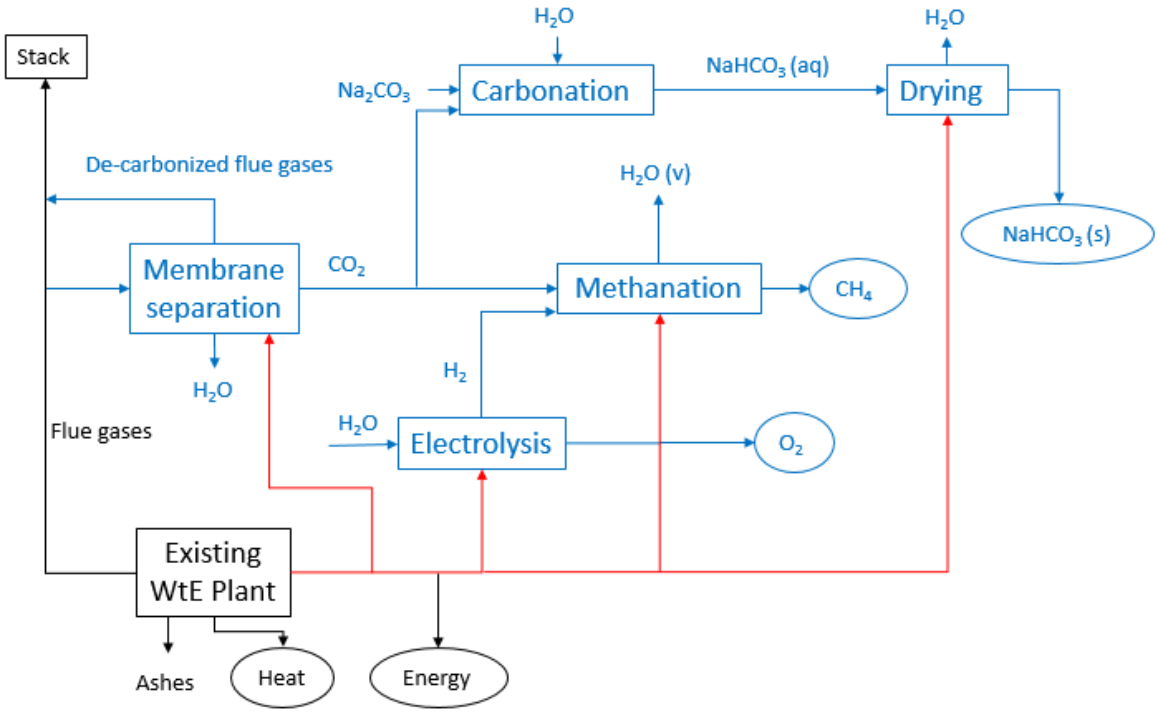

Figure 9. Process Flow Diagram of the desired scenarios by TERSA

Any power-to-gas route needs hydrogen to react with CO_2. As mentioned in the state-of-the-art, if hydrogen is desired to be cataloged as green, renewable electricity shall be used to feed the

electrolyzer. In the TERSA case study, two energy sources are taken into account: electricity produced in the current turbines of the WtE plant; and photovoltaic panels (PV). PV panels are an attractive technology because of the availability of surface area within the plant footprint and its sunny location in Barcelona.

In order to guide the reader through all the different scenarios presented in this case study, Figure 10 contains a simplified scheme of the different process routes (straight boxes) that have carbon capture (round box) in common. Bicarbonate scenario, which will be referred to as Scenario 1, is furtherly divided into two sub-scenarios, dry bicarbonate and bicarbonate slurry. Bio-methane scenario will be referred to as Scenario 2.

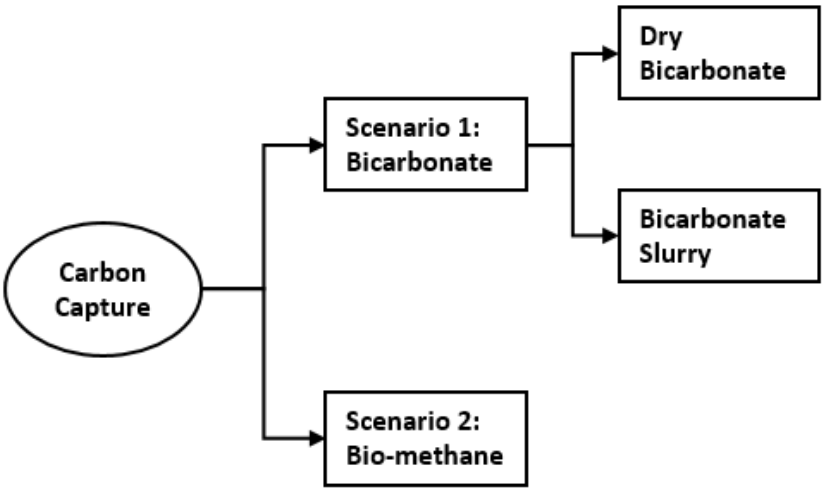

Figure 10 Simplified scheme of the different alternative scenarios of this case study

The following pages explain the methodology used in the formulation of mass balances and economic analysis. Afterwards, all scenarios studied are explained in detail.

3.1. Methodology

Mass balances were calculated by adapting literature data with the data provided by TERSA. The goal of this part was to extract the necessary data to feed a preliminary cost estimate. The economic estimation of package units such as the electrolyzer, carbonation tower and methanation section were calculated from Equation (5) using existing data of similar plants when possible. In the case for heavily patented technologies that did not have many references available, like the spray dryer, a preliminary quotation was requested to *GEA Niro*. Finally, the CAPEX of basic equipment, such as vessels, compressors and membranes, was calculated through the bare module cost algorithm as follows [50]:

- Estimate C_p^0 for the desired piece of equipment through Equation (22). This is the purchased equipment cost for the base case (carbon steel construction and near ambient pressure).

$$\log_{10} C_p^0 = K_1 + K_2 \log_{10}(A) + K_3[\log_{10}(A)]^2 \quad (22)$$

where A is the capacity or size parameter for the equipment and K_1, K_2 and K_3 are constants.

- Find the correct relationship for the bare module factor for vessels according to Equation (23).

$$C_{BM} = C_p^0 \cdot F_{BM} = C_p^0 \, (B_1 + B_2 \, F_M \, F_P) \quad (23)$$

- Find the pressure factor, F_P, and the material factor, F_M, for vessels to calculate F_{BM} according to Equation (23).
- For other equipment, find the bare module factor, F_{BM}.
- Calculate the bare module cost of equipment, C_{BM}.
- Escalate the cost to the present year by using the Chemical Engineering Plant Cost Index (CEPCI) from 2001 (CEPCI-397) to 2017 (CEPCI-567.5) [51].

$$C_2 = C_1 \left(\frac{I_2}{I_1}\right) \quad (24)$$

where C = Purchased cost; I = Cost Index.

- Calculate the total module cost (C_{TM}) to consider the contingency cost and fees (15% and 3% of the bare module cost respectively).
- Calculate the grass root costs including the auxiliary equipment needed to operate the main machinery. These costs are assumed to be equal to 50% of the bare module costs for the base case conditions.

When estimating the yearly production costs, the CAPEX was annualized using the Capital Recovery Factor (CRF) during the plant life time according to Equation (25) [30]:

$$C_{CAPEX} = C \cdot CRF(N, i) = C \cdot \frac{i \, (1+i)^N}{(1+i)^N - 1} \quad (25)$$

where C is the Total Capital Cost, N is the Economic plant life time (20 years) and i is the interest rate (5%).

Maintenance and labor costs were also taken into account in the OPEX of all scenarios. Maintenance costs were assumed to be 6% of the capital expenses [50]. One additional operator per production line (membrane separation, bicarbonate production and methanation) was assumed to be required. Since the plant is operated in steady-state, three 8h shifts were considered. Gross expenses per operator

and shift of 30000 EUR/y were taken into account. Also, the plant is expected to be operated 8299 h/y, the same average time that the furnaces worked in 2019 [52].

In case the reference values are given in USD, the used exchange ratio for all calculations is 1.2 USD/EUR. All costs are reported in EUR.

After the technical analysis of the different scenarios, an economic estimate of their respective cost will be carried out. Three main parameters will be obtained to compare them: CAPEX, OPEX and savings in comparison with the current scenario. Also, the annualized CAPEX, using the CRF, will be summed with the OPEX to obtain the total annual costs for each alternative. The better option will be the one that has the bigger revenues, which are calculated by the difference between annual savings and costs.

3.2. Scenario 1: Sodium bicarbonate production

Usually, bicarbonate is dried using a centrifuge and a vertical tube dryer [46]. However, any WtE plant has lots of hot air in excess that potentially could be used to dry the bicarbonate slurry in a process called spray drying. This drying technology is mainly used in the food and pharmaceutical industry. There are some patents such as Solvay's WO2014096457 [53] and WO2007109885 [54] that use spray drying (or atomization) to produce fine powder sodium bicarbonate, in the range of hundreds of microns of particle diameter, from bicarbonate slurry. According to Solvay, the optimal sodium bicarbonate particle diameter is around 40 µm [55]. Since this technology is largely patented, there are not many open reports addressing this topic. This is why a specialized vendor was reached out, *GEA Niro*.

With more than 3000 references for spray drying plants for R&D and small production units, *GEA Niro* has the expertise of spray drying technology required. However, after reaching out to their technical team, *GEA Niro* did not have any reference of any spray drying working with bicarbonate slurry. Their product portfolio, such as their *CONTACT FLUIDIZER* ™ and flash dryers, work with slightly moist solid feeds. Before the final drying step, the bicarbonate slurry is usually crystallized in a conventional dryer. Then, the formed crystals are separated in a centrifuge.

Although the state-of-the-art operation for producing solid bicarbonate from slurry includes the drying and centrifuging steps, *GEA Niro* performed a pilot plant test in which sodium bicarbonate slurry was directly dried in a *VERSITALE-SD-28* ™ spray dryer. The resulting particles were found to be empty with an average particle size of 60-70 microns. It was also observed that, as a consequence of the drying temperature, some fraction of bicarbonate was lost due to sodium carbonate formation by reversing reaction (11). Working in an inert atmosphere rich in CO_2 was recommended by *GEA Niro* to reduce the carbonate formation. Thus, the conclusion after contacting the vendor was that if solid bicarbonate

is produced, a dryer, centrifuge and spray dryer are needed, representing a significant impact in the CAPEX of the project. The alternative is to use the bicarbonate slurry without drying as it is being done in Twence facility [44], which already would be an improvement of the current process which uses CaO slurry. Another option is to delete the last spray drying unit since the moisture after the first dryer and centrifuge was reported to be less than 0.05% in similar plants [45]. Since sodium bicarbonate is used as a bulk reagent, the effort of decreasing even furtherly the moisture content is not correlated with its benefits. To sum up, the advantages of having a dry product are better handling of the material, which can save some money in maintenance, mass reduction and avoidance of reintroducing water in the furnace. Whereas the disadvantages are increasing both CAPEX and OPEX due to the need of more process units and the increase of electrical consumption.

3.2.1. Mass balance of Sodium bicarbonate unit

The overall sodium bicarbonate production route is schematized in Figure 11. The first step is the dilution of sodium carbonate, which is usually purchased and stored in solid form. The storage equipment, such as silos and vessels, that are currently being used for quicklime could be reused for carbonate. Afterwards, the soda ash is carbonated with the captured CO_2 to produce bicarbonate slurry in a carbonation tower (or carbonator).

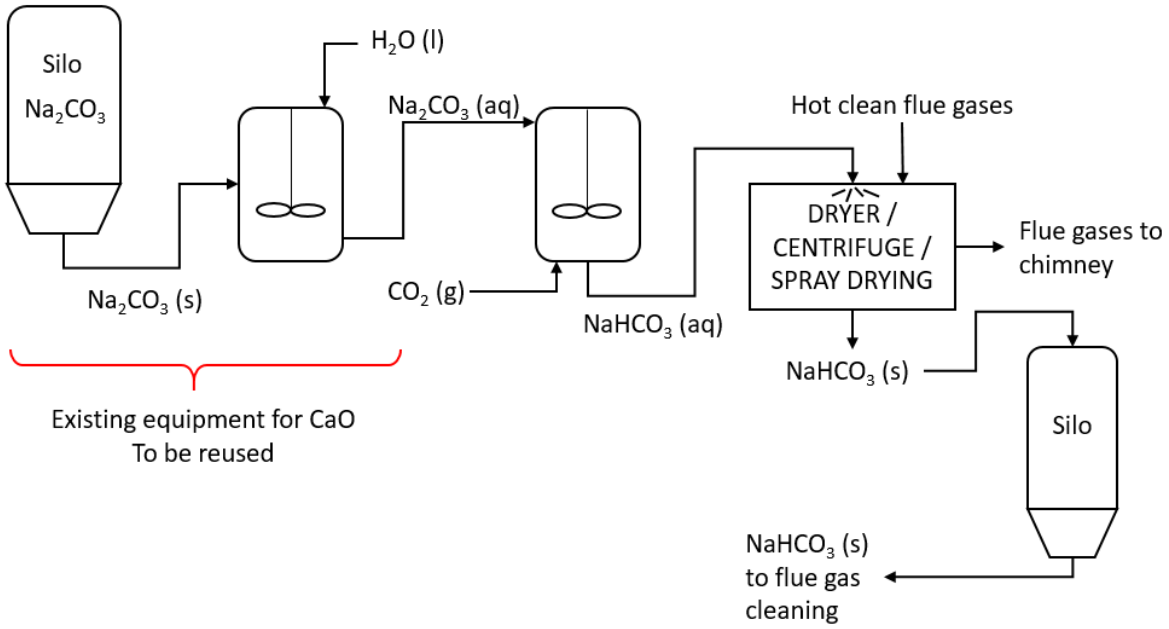

Figure 11. Scheme of the sodium bicarbonate production route

TERSA foresees a powder sodium bicarbonate demand of 100 kg/h in dry basis per furnace, which in total sums **300 kg/h** in total if the three furnaces are in operation at the same time. Therefore, following the stoichiometric ratio of the carbonation reaction, assuming a 90% Na_2CO_3 conversion [44] and 5%

bicarbonate losses in the spray drying step, the required sodium carbonate carbon dioxide and water demand can be calculated as described by Equations (26)-(28):

$$\dot{w}_{Na2CO3} = \frac{300\ kg\ NaHCO_3(s)}{h} \cdot \frac{100\ kg\ bicarb.}{95\ kg\ NaHCO_3(s)} \cdot \frac{1\ kmol\ bicarb.}{84\ kg\ bicarb.} \cdot \frac{1\ kmol\ Na_2CO_3\ reac.}{2\ kmol\ bicarb.} \cdot \frac{100\ kmol\ Na_2CO_3\ feed}{90\ kmol\ carb.reac} \cdot \frac{106\ kg\ Na_2CO_3}{1\ kmol\ Na_2CO_3} = 222\ {}^{kg\ Na_2CO_3\ (s)}/_{h} \quad (26)$$

$$\dot{w}_{CO2} = \frac{300\ kg\ NaHCO_3(s)}{h} \cdot \frac{100\ kg\ bicarb.}{95\ kg\ NaHCO_3(s)} \cdot \frac{1\ kmol\ bicarb.}{84\ kg\ bicarb.} \cdot \frac{1\ kmol\ CO_2}{2\ kmol\ bicarb.} \cdot \frac{44\ kg\ CO_2}{1\ kmol\ CO_2} = 83\ {}^{kg\ CO_2}/_{h} \quad (27)$$

$$\dot{w}_{H2O} = \frac{300\ kg\ NaHCO_3(s)}{h} \cdot \frac{100\ kg\ bicarb.}{95\ kg\ NaHCO_3(s)} \cdot \frac{65\ water}{35\ kg\ bicarb} + \frac{300\ kg\ NaHCO_3(s)}{h} \cdot \frac{100\ kg\ bicarb.}{95\ kg\ NaHCO_3(s)} \cdot \frac{1\ kmol\ bicarb.}{84\ kg\ bicarb.} \cdot \frac{1\ kmol\ water\ reac.}{2\ kmol\ bicarb.} \cdot \frac{18\ kg\ H_2O}{1\ kmol\ CO_2} = 620\ {}^{kg\ H_2O}/_{h} \quad (28)$$

The ratio between CO_2 and $NaHCO_3$ produced is very close to the one reported by Twence (4 kg NaHCO3 per 1 kg CO_2), which validates the overall reaction system.

3.2.2. Economic analysis of Sodium bicarbonate unit

Although techno-economic data is scarce in literature because this technology is still involved in on-going patents, similar plants had been designed and conceptual data is available. For example, a CO_2 mineralization process was studied by Lee et al. [45] (Korea Advanced Institute of Science and Technology, KAIST, 2019), where flue gases from a coal-fired power plant were used to produce sodium bicarbonate via soda ash carbonation, including a dewatering and drying post-treatment to obtain baking soda in powder form [45]. Even though the duty and the overall process scheme of this plant is not the same as the TERSA case study, it can be used to have a cost estimation of the carbonation step, since this technology is common for both cases. The KAIST plant, with a production capacity of 3400 kg $NaHCO_3$ (s) per hour, had an estimated CAPEX for the carbonation reactor of 417 kUSD and 1757 kUSD for the dryer and centrifuge. Following the economic scale-up heuristic of the six-tenths rule [36] in Equation (5), the CAPEX for the carbonation unit at TERSA, without considering the spray dryer, was estimated as in Table 8:

Table 8. Economic estimate of the carbonator

KAIST $NaHCO_3$ capacity (kg/h)	**3400**
KAIST carbonator + dryer CAPEX (kUSD)	2174
TERSA yearly production	8299 h/y
TERSA $NaHCO_3$ capacity (kg/h)	300
Estimated TERSA carbonator C_{BM} (kEUR)	89.6
Estimated TERSA dryer system C_{BM} (kEUR)	453

The dry baking soda production in the carbonator already considers 5% product loss during the drying step, which is designed to produce 315 kg/h of dry sodium bicarbonate. Additionally, a new silo is needed to store a minimum buffer quantity of sodium bicarbonate in case the dryer needs some maintenance. The WtE furnaces operate 24 h/d and need some back-up of a critical raw material used in the cleaning stage of the flue gases. A metallic silo of capacity for storing the equivalent consumption of one day of solid sodium bicarbonate was added to the study.

Considering the design consumption of 315 kg/h of sodium bicarbonate and a bulk density of 977 kg/m^3 [56], the volume of the silo was calculated by Equation (29):

$$V_{NaHCO3\ Silo} = 315\,\frac{kg}{h}\cdot\frac{1\,m^3}{977\,kg}\cdot 24\,h = 7.73\,m^3 \tag{29}$$

The final design volume of the silo was taken as **10 m^3** to have some space available. According to Turton's Handbook [50], the cost estimate factors for vertical process vessels are list in Table 9:

Table 9. Equipment cost data for atmospheric carbon steel vertical pressure vessels [50]

K_1	K_2	K_3	B_1	B_2	F_P	F_M
3.4974	0.4485	0.1074	2.25	1.82	1	1

The pressure factor for atmospheric vertical vessels is 1, so the sodium bicarbonate silo it is not being affected by this factor. The construction material for the silo was assumed to be carbon steel which has a material factor of 1 as well. Using the factors of Table 9 into Equations (22) and (23) led to the resulting bare module cost included in Table 10:

Table 10. Economic estimation of sodium bicarbonate silo

C_p^0 (USD)	F_{BM}	C_{BM} (USD, 2001)	C_{BM} (USD, 2017)
11,306	4.07	46,014	65,776

The dried bicarbonate case has an extra cost related to the additional centrifuge, its electrical consumption. The power demand of the centrifuge was calculated by scaling down the KAIST [45] process by the six-tenths rule. As a result, the centrifuge was expected to consume annually 385 MWh, which supposed an OPEX of 14270 EUR/y.

In case that the bicarbonate slurry is not meant to be dried, an intermediate storage vessel is also required to meet the same function as the silo. Since the slurry contains water, the increase of the product density is balanced with the fact that there is less amount of bicarbonate in the same quantity of product. Taking into account an average slurry density of 1500 kg/m^3, the required volume was 13 m^3. The final design volume for the vessel was increased using the same factor as for the silo case. Then, an 18 m^3 vessel was needed for the intermediate storage of the bicarbonate slurry. The equipment cost data was also taken from Table 9, which gave a bare module cost of 98,717 USD adjusted with the 2017 CEPCI.

Either if the sodium bicarbonate is dried or not, both sub-scenarios replace the current use of CaO with Na_2CO_3. Quicklime is being purchased by TERSA at 73 EUR/t. Then, the avoidance of this raw material is considered as a saving. The estimated purchase cost of sodium carbonate was assumed to be 220 EUR/t [57]. Changing the cleaning agent to bicarbonate has other benefits that are not countable. The reduction on the maintenance costs and the improvement of the performance are two examples of it. As a consequence, the increase of the raw material cost from CaO to sodium carbonate is expected to have a huge impact in the cost analysis.

3.3. Scenario 2. Bio-methane production

The bio-methane production route uses both captured carbon dioxide from the membrane unit and hydrogen from the electrolyzer. The two streams are already compressed at the required pressure, so the methanation section scope goes from the merge of the two pressurized CO_2 and H_2 feed streams until the condensation of steam and storage of CO_2 into a pressure vessel. The produced bio-methane is used in the three existing furnaces to control the incineration temperature as well as a starting ignition source for the inlet waste. The goal of producing bio-methane from the captured CO_2 is replacing the current scenario of gas natural injection into the furnaces. If this natural gas (95% vol. methane) is produced in-house, the circularity of the new overall process is enhanced. Moreover,

depending on the gas natural price and the costs of this new unit, this solution could even be economically profitable.

3.3.1. Methanation stage

3.3.1.1. Mass and energy balances of Methanation unit

The core of this process is the methanation reactors section where catalytic conversion of CO_2 and H_2 into SNG is achieved. However, before reaching the methanation reaction, oxygen shall be removed from the rich CO_2 stream after carbon capture. Oxygen reacts with hydrogen through the extremely exothermic water formation reaction (30):

$$H_2\,(g) + {}^1\!/_2\,O_2\,(g) \rightarrow H_2O\,(l) \qquad \Delta H_{298\,K} = -241.8\ kJ/mol\ \text{(l)} \tag{30}$$

If this reaction occurs in the methanation reactor, the resulting high temperature could damage the catalyst and, therefore decreasing the CO_2 conversion [30]. As a consequence, residual oxygen needs to be removed upstream methanation stage, in a so-called de-oxo stage. A basic process flow diagram of the de-oxo stage is shown in Figure 12.

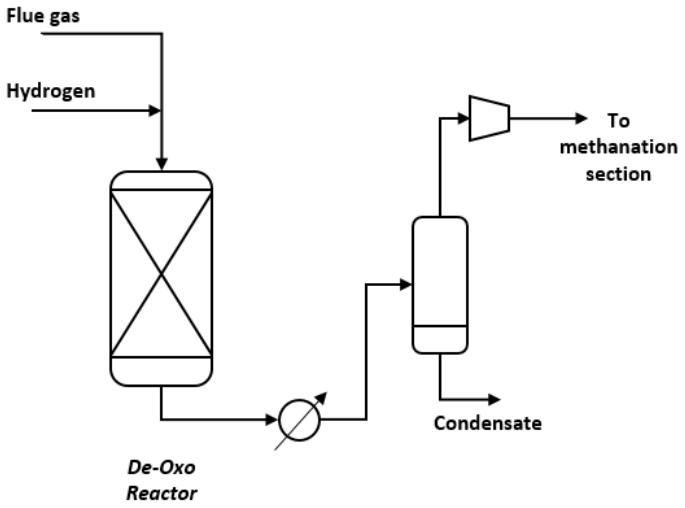

Figure 12. Process flow diagram of de-oxo section [30]

Figure 13 shows the process flow diagram of this section including three adiabatic fixed-bed reactors with intercooling. Operating temperature was selected taking into account that too low temperatures, although they are favorable from a thermodynamic point of view, cause kinetics limitation. On the other hand, under too high temperatures, catalyst integrity could become an issue and the reverse reaction gains predominance. Thus, operating conditions were selected not to exceed 500 °C [30].

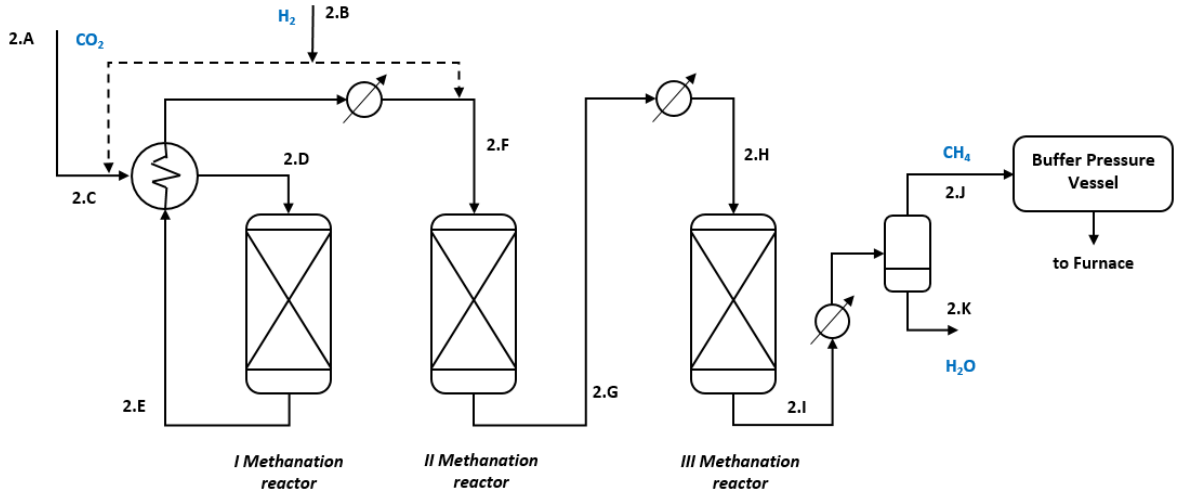

Figure 13. Process flow diagram of methanation section [30]

The overall reaction (2) is exothermic and, as a consequence, output streams could be used to preheat the reactor feed to increase the energy efficiency of the process. Figure 14 shows the evolution of CO_2 conversion through the three adiabatic reactors in series. The first two reactors account for the majority of CO_2 conversion without exceeding the equilibrium line. *Methanation reactor I* works with lower H_2/CO_2 ratio than the overall (solid line) in order to work inside the defined temperature range. After it, more hydrogen is injected into the system before *Methanation reactor II* to correct the reactants ratio to work within the dashed line inside a safe temperature range. Finally, although *Methanation reactor III* has the lowest contribution to the overall conversion, it allows reaching a carbon conversion of 100%.

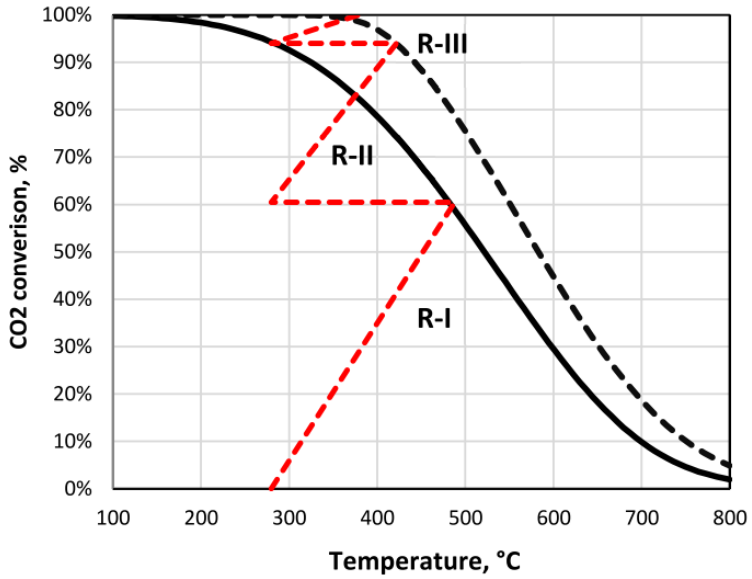

Figure 14. Evolution of CO_2 conversion in the multi-reactor configuration: solid line = partial H_2/CO_2 ratio, dashed line = overall H_2/CO_2 ratio [30]

To sum up, the overall methanation section works with a stoichiometric H_2/CO_2 ratio of 4 and reaches a CO_2 conversion of 100%. Main operation pressures and temperatures are shown in Table 11. This data was used to compute the cooling water needs for this section, which makes up for part of its OPEX.

Table 11. Operating pressures and temperatures of the methanation reactors

Stream ID	**2.D**	**2.E**	**2.F**	**2.G**	**2.H**	**2.I**
P (atm)	5.0	4.8	4.6	4.4	4.3	4.1
T (°C)	280	499	280	421	280	297

The methanation section ends with the separation of bio-methane and steam in a total condenser. The high conversion and the fact that the feed ratio is stoichiometric, makes this reaction free of undesired by-products. Finally, the bio-methane is stored in an intermediate buffer pressure vessel before being injected in one of the three operating furnaces whenever required.

Considering a carbon conversion of 100% due to the use of three adiabatic reactors in series, a stoichiometric CO_2/H_2 ratio, and a natural gas consumption of **45000 Nm^3/month** of natural gas declared by TERSA, the methanation inlet and outlet main parameters were calculated and summarized in Table 12.

Table 12. Methanation section black box mass balance

	Inlet		**Outlet**	
	CO_2	H_2	CH_4	H_2O
Flowrate (kg/h)	121.5	22.1	44.18	99.4

Heat exchangers are used to lower the temperatures of the reactor products before entering to the next reaction stage and to condensate the steam produced. Cooling water is supplied at 20 °C to remove the heat excess. The heat transfer equipment were sized to return the cooling water at 50 °C. Then, using the conversions and temperature requirements of the three reactors, and the mass balance the total demand of cooling water was calculated using HYSYS. The simulation outcome showed a cooling water consumption of 27000 m^3/y.

After the total condenser, 44.18 kg/h of almost pure methane at 3.9 atm are stored into a horizontal pressure vessel. The vessel was designed to have the equivalent consumption of bio-methane for one day. Compression of bio-methane was not considered because, although it would require less volume,

it would fire back in the compression costs. A quick sizing of the vessel was done using HYSYS, resulting in a volume requirement of 18.75 m^3 which was traduced to a design volume of 25 m^3 to round it up.

3.3.1.2. Economic analysis of Methanation unit

For the CAPEX estimate, the methanation reaction section was considered as a package unit. The scope of this package includes the reactors, heat exchangers and condenser. Iaquaniello et al. [30] proposed a methanation plant fed with post-combustion flue gases without carbon capture (direct methanation). Economic data was adapted from this study and the plant capacity was standardized using the feed flowrate that enters the first methanation step. The estimation was done following the six-tenths rule [36]. Table 13 shows the results of the CAPEX estimate of the package.

Table 13. Economic estimation of the methanation package (reactors, heat exchangers and condenser)

Direct methanation capacity. Feed (kmol/h)	**6400**
Direct methanation CAPEX (EUR)	64,800,000
Estimated TERSA capacity. Feed (kmol/h)	8.3
Estimated TERSA CAPEX (EUR)	1,199,000

The only equipment that is not included within the package is the 25 m^3 bio-methane vessel. The method used is the same as for the sodium bicarbonate silo [50]. The main differences between the two vessels are that the bio-methane one is horizontal rather than vertical; the pressure factor F_P was considered taking into account P = 3.9 atm and an estimated diameter, calculated from the quick sizing function of HYSYS, of D = 2.77 m; and the material was stainless steel to avoid pickling of the tank, which increases the material factor F_M.

While Table 14 compiles all the data used in this CAPEX estimation, Table 15 shows the final cost of the equipment.

Table 14. Equipment cost data for stainless steel horizontal pressure vessels, P = 3.9 atm, D = 2.77 m [50]

K_1	K_2	K_3	B_1	B_2	F_P	F_M
3.5565	0.3776	0.0905	1.49	1.52	1.79	3.1

Table 15. Economic estimation of the bio-methane buffer vessel

C_p^0 (USD)	F_{BM}	C_{BM} (USD, 2001)	C_{BM} (USD, 2017)
18 248	9.90	180 689	258 290

As mentioned beforehand, methanation stage includes heat exchangers that operate with cooling water. The utility costs were given by TERSA (0.576 EUR/m^3). Then, the OPEX of the methanation, considering cooling water, was about 15,533 EUR/y.

The savings of methanation comes from the avoidance of natural gas purchase. At the moment, TERSA pays 0.55 EUR/Nm^3 of natural gas. Similarly than in Scenario 1 (bicarbonate production), substituting the raw material for an in-house production was counted in the profit and losses balance.

3.3.2. Electrolyzer unit for hydrogen production

The electrolyzer unit is needed to supply the required hydrogen to the methanation reaction. Then, the sizing of this equipment is related to the demand of the downstream unit. The scope of the electrolyzer unit starts with the electricity and water intake, and ends at the hydrogen and oxygen outlet of the electrolyzer. It was assumed that both gases leave the electrolyzer with more than the required pressure for the next stages [48]. The electricity used shall be green if the process is desired to be kept under the net negative carbon emissions frame. As a consequence, two alternative energy sources were considered for this unit: solar energy from new installed PV panels in an available surface of **160 m^2**, and electricity produced in the same WtE plant which is currently being sold. Using electricity produced in the WtE is considered a penalty since the revenues from electricity sales will decrease. The oxygen was considered as a sub-product to be sold in order to optimize the economic performance of the plant. Figure 15 provides an overview of the hydrogen production stage. The units marked in red exist in the current WtE plant.

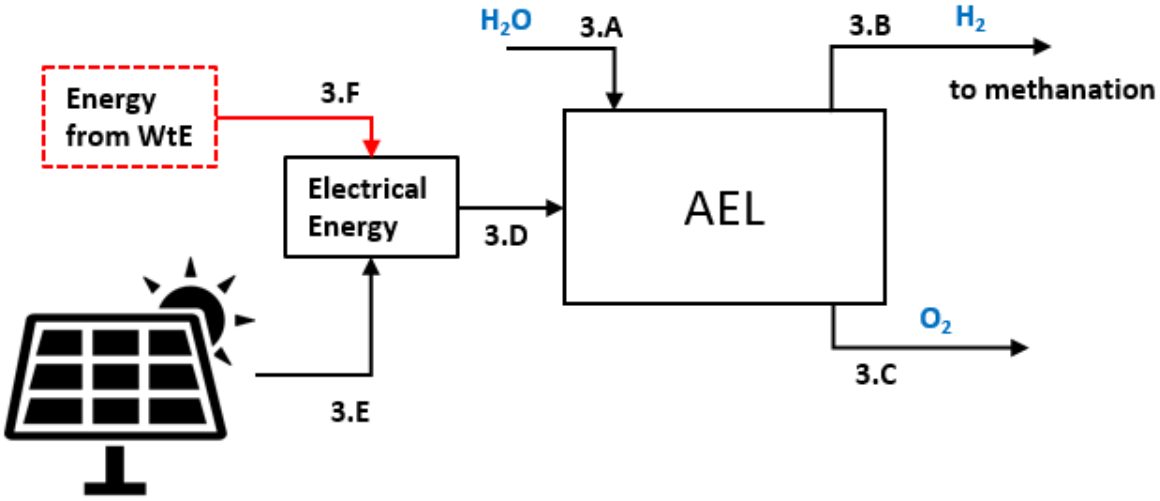

Figure 15. Electrolyzer unit overview

The hydrogen demand is the factor that sizes the electrolyzer. As it had been explained in the state-of-the-art chapter, currently alkaline electrolysis (AEL) is the most mature technology. In addition, it is the best positioned in economic terms as well. Although PEMEL systems is expected to surpass this technology in the near future, the advantages of PEMEL are related to a flexible operation. Having short start-up times is key when the electrolyzer is designed to be operated only when the price of electricity is attractive. However, the purpose of this unit is to work continuously as much as possible to keep the production of hydrogen, and therefore bio-methane, constant over time. At the end, the technology selected was AEL because its lower CAPEX in comparison with PEMEL.

3.3.2.1. Mass and energy balances or Electrolyzer

The AEL is a package unit and was considered a black box in terms of its design. The water feed is demineralized in the same electrolyzer skid. The main design parameters such as unit efficiency are summarized in Table 16 [58].

Table 16. Electrolyzer main design parameters [58]

H_2 demand to methanation (kg/h)	**22.1**
HHV H_2 (kWh/Nm^3)	4.8
AEL energy efficiency	74%
Electricity demand (kW)	1604
Demineralized water demand (L/h)	200

By-product O_2 production (kg/h)	176.7

A preliminary simulation of a sub-scenario in which the energy is produced in situ by PV solar panels was studied. *PVSyst* software was used in this case considering the location of the plant and the approximate sun irradiation parameters. TERSA declared having an available surface of 160 m^2 to install PV panels. Table 17 summarizes the principal outcomes of the study.

Table 17. Results of the PVSyst simulation for the PV panels sub-scenario

Available surface (m^2)	**160**
Annual energy provided (kWh)	33520
PV installed peak power (kWp)	21.6
Solar power to electrolyzer demand ratio	0.25%

A first estimate indicates that the available surface is not enough to cover for the electrolysis demand. Only 0.25% can be covered with PV panels. The rest is assumed to come from the existing WtE plant. In the year 2019, TERSA sold 171173 MWh of electricity to the grid [52], which represents 8% of the electrolyzer demand. Although the energy penalty fraction is big, it is better to use in-house electricity because it is cheaper than purchasing it and a fraction of it comes from biogenic waste. Usually, solar panels are coupled with batteries that are charged during over-production hours and discharged when the demand is higher than the production. In this case, batteries can be neglected because the electrolyzer demand will never be supplied with only PV panels. The maximum power provided in a summer day is 21.6 kW, which falls short if the electricity demand for the electrolyzer is 1.6 MW as it is indicated in Table 16.

To put the PV panels' performance into perspective, the *Pèrgola del FORUM*, which is also owned by TERSA, has an area of 3410 m^2 that provides a nominal power of 375 kW [59]. If the same PV technology would be used to feed the electrolyzer an area of 14585 m^2 would be required. This is approximately the total area of two football pitches. Thus, it is clear that any solar power system needs a huge amount of space that will never fit inside the current TERSA facility. However, this sub-scenario was taken into the economic analysis step to compute the turnover of the inversion. It was expected that the initial investment of the PV panels overcome the electricity price at any time in the future, making the investment attractive.

3.3.2.2. Economic analysis of Electrolyzer

The economic analysis of both the electrolyzer unit and the PV panels' sub-scenario were also simplified following the black box philosophy. The main parameters are shown in Table 18. By combining the data from the mass and energy balances with this one, an approximate CAPEX and OPEX was obtained.

Table 18. Main parameters of the economic estimation of the electrolyzer and PV panels

CAPEX AEL @ 1.6 MW (EUR/kW)	**800**	**[58]**
Water costs (EUR/month)	250	[60]
WtE electricity selling price (EUR/MWh)	44.5	(TERSA)
CAPEX PV (EUR/Wp)	0.46	[61]
OPEX PV (EUR/kWp/a)	9.2	[61]

The water costs estimate considers contracting the supply to *Aigües de Barcelona* [60] of a nominal flowrate of 0.40 m^3/h.

3.4. Carbon Capture with membrane technology

Both sodium bicarbonate and bio-methane production scenarios are fed with CO_2 that is captured from the flue gases of the WtE plant. The selected technology was Polaris Gen-2 membranes from MTR [22]. These membranes are the second generation of the Polaris™ Project from *MTR* and are being tested in a pilot plant scale with a capacity similar to the one of this study [22]. These membranes consist of an active polymeric separation layer coated on an ultrafiltration membrane cast on a non-woven support paper. The active layer is selective for polar gases such as CO_2. The reference parameters for this membrane can be found in Table 19. Two set of membranes operate in series to purify the permeate rich in CO_2. The flue gas to be treated are composed mainly in N_2, H_2O, O_2 and CO_2 according to Table A1 of the Annex

Table 19. Main membrane parameters of Polaris Gen-2 membranes [22]

Permeance (GPU)	**2000**
CO_2 / N_2 selectivity	49
O_2 / N_2 selectivity	2.3

T (°C)	38

It is important to remark that, currently, the methanation and carbonation processes do not require a high purity of CO_2 [30], [45]. However, this has an impact in the costs distribution. Although the costs related to the carbon capture stage are avoided, working with a lower CO_2 concentration requires handling a bigger total flowrate. Thus, the equipment shall be scaled-u to fit the increase of flue gases flow. This also has consequences in the OPEX, since the compressors would consume more electricity. This alternative of direct methanation and carbonation (without carbon capture) will be discussed briefly in Chapter 4.4. Some qualitative conclusions can be drawn from the distribution of the costs.

3.4.1. Mass and energy balances of Carbon capture

The carbon capture unit starts with the compression of the feed flue gases. The gases are cooled down to the operating temperature of the membranes (38 °C) and the condensed water is removed in a total condenser. The recovered pure water is re-used in the sodium bicarbonate step. By doing so, the total water consumption of the plant is reduced. The dry gases enter the first stage of membranes at 8 bar to recover 90% of the feed carbon. The retentate side is low on carbon and can be vented to the atmosphere. Before that, the gases are still at a significant pressure. A 10% pressure drop was assumed for the retentate, this stream is circulated at 7.2 bar to an expander to recover a fraction of the compression energy. The permeate leaves the membrane stack at 1 bar and is re-compressed to 3 bar before going through the second membrane stage. Again, 90% of the carbon passes to the permeate side, which ends up with a 96.5% volumetric fraction of CO_2. The retentate is recirculated back to the first stage to increase the CO_2 concentration of the feed gases. Finally, the rich-CO_2 stream is compressed to the feed pressure of the methanation unit, 5 bar. The process flow diagram of this stage is shown in Figure 16.

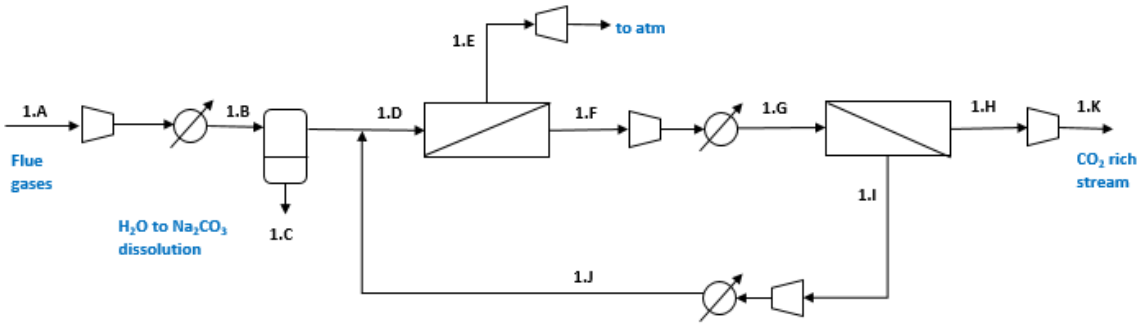

Figure 16. Process flow diagram of the carbon capture unit

Membranes, compressors and the expander were the equipment sized in this section. Membrane area was calculated using the permeance, selectivity, flowrate and composition of the feed and permeate according to Equation (31).

$$J_i = \frac{Q_{Perm,i}}{A\left(P_{Feed} \cdot X_{i,Feed} - P_{Perm} \cdot X_{i,Perm}\right)} \quad (31)$$

where J_i = Permeance component i; $Q_{Perm,I}$ = Component I flowrate in the permeate; A = membrane area; P_{Feed} = Feed pressure; P_{Perm} = Permeate pressure; $X_{i,Feed}$ = molar fraction of component i at the feed; $X_{i,Perm}$ = molar fraction of component i at the permeate.

Compressor and expander duty (kW) were calculated according to Equations (32) and (33) respectively [62].

$$E_{comp} = \frac{F}{\eta}\frac{\gamma RT}{\gamma - 1}\left[(\psi)^{(\gamma-1)/\gamma} - 1\right] \quad (32)$$

$$E_{exp} = \eta\, F\, \frac{\gamma RT}{\gamma - 1}\left[1 - (1/\psi)^{(\gamma-1)/\gamma}\right] \quad (33)$$

where η is the adiabatic efficiency of both compressor and expander which was assumed to be 75%, ψ is the pressure ratio across the equipment and γ is the adiabatic expansion factor which was assumed to be 1.37.

At this point, once all parameters are defined, the equation system is left with only two unknowns, feed flowrate and membrane areas. Since the final CO_2 permeate flowrate is given as the demand of the bicarbonate and methanation units, the inlet flowrate of raw flue gases to be treated is known. Thus, the membrane areas is calculated according to Equation (31). The composition at any point of the capture system only depends on the pressure, the selected carbon rejection ratio and the intrinsic parameters of the membrane (permeance and selectivity). These common parameters for all scenarios are summarized in Table 20.

Table 20. Composition and pressure of the main streams in carbon capture unit

Stream ID	X CO_2	X N_2	X O_2	X H_2O	P (bar)
1.A	0.0878	0.6294	0.0999	0.1829	1
1.D	0.1100	0.7609	0.1290	0.0000	8
1.E	0.0131	0.8529	0.1340	0.0000	7.2

1.G	0.6180	0.2792	0.1028	0.0000	3
1.K	0.9668	0.0182	0.0150	0.0000	5
1.I	0.1455	0.6328	0.2217	0.0000	2.7

Depending on the CO_2 demand of each scenario, the membrane area, compressors and expander duty were re-calculated to fit the process needs.

3.4.2. Economic analysis of Carbon capture

The principal economic parameters of this section are the capital costs of purchase of membranes, compressors and the expander. Membranes were expected to last for 5 years, whereas the project lifetime was set at 20 years. The CAPEX for membranes was assumed to be 50 USD/m^2 [22], [62]. The compressors and expander CAPEX was calculated according to the bare module cost algorithm [50]. Cost data can be found in Table 21 for these two components.

Table 21. Equipment cost data for compressors and expanders [50]

	K_1	K_2	K_3	F_{BM}
Compressor	2.289	1.36	-0.1027	2.15
Expander	2.2476	1.4965	-0.1618	3.5

When it comes to the OPEX, electric consumption is the major cost. It depends on the energy consumption of the compressors and the power recovered by the expander. The price of electricity was set, as in the previous cases, at the current selling price of the produced electricity in the WtE plant. The replacement of membranes was considered as well in the OPEX but has a minor weight in comparison with electricity costs.

4. Results and discussion

In this section, the results of the different scenarios are discussed. Whereas the technical feasibility of the project has been proven in the previous pages, the total inversion needed to make this project are explained herewith.

Besides the principal scenarios already presented, each one has additional internal alternatives, such as installing PV panels to provide electricity to the electrolyzer and using an expander to recover some energy from the retentate stream of the first membrane stack. The main KPIs used to discuss the economic results were the CRF and the payback time of the inversion. Commonly for all scenarios, the interest rate and lifetime of the project were assumed to be 5% and 20 years respectively.

4.1. Scenario 1: Sodium bicarbonate scenario

Sodium carbonate scenario has two main alternatives: producing a 35 %wt slurry or obtaining the sodium bicarbonate in dry powder form. After contacting with *GEA Niro,* the slurry drying operation considered a dryer, to eliminate the major part of moisture, and a centrifuge to separate the powder crystals formed. The resulting powder has around 0.05% of moisture [45], which can be considered dry enough since this product is meant to be re-used in the same plant. As it was explained before, the additional equipment to completely dry the bicarbonate particles was deleted. As a consequence, the KAIST set-up (drier and centrifuge) and the slurry sub-scenarios (Twence configuration) were compared.

The CAPEX of the two sub-scenarios is the same up to the exit of the carbonator tower. The CO_2 required in the two systems is equal because the dry mass of sodium bicarbonate that is produced does not change. The only difference remains in the water content. As it is shown in Figure 17, the main capital cost difference is the purchase of the dryer and centrifuge packages, with an estimated cost of 634 kEUR for both. The storage for the slurry sub-scenario is more expensive because of the lower bicarbonate density in solution due to the high content of water (65%wt). However, this additional cost is only about 45 kEUR. Thus, drying the bicarbonate increases the CAPEX of Scenario 1 by a factor of 2.

Even though the costs difference is huge when only the initial investment is considered, Figure 18 and Figure 19 show the total annualized costs for the two sub-scenarios. The annualized costs take into account both the CAPEX and OPEX. This allows comparing the two solutions and obtaining the average total costs in annual basis.

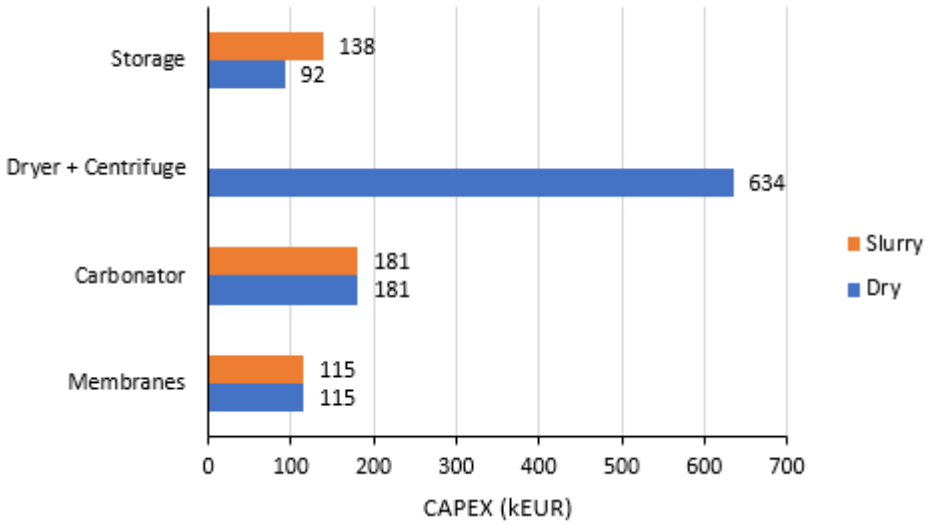

Figure 17. CAPEX comparison of dry and slurry bicarbonate sub-scenarios

Besides the difference on the equipment purchase costs, as seen in Figure 17, other aspects increase the annual costs of the dried solution in comparison with the slurry one. The electric consumption of the centrifuge, which is unique for the drying step, supposes an additional 34 kEUR per annum. In addition, since maintenance costs were estimated to be a function of the total fixed costs, they also increase for the dry sub-scenario. Given that the equipment purchase costs are doubled, the maintenance costs are also multiplied by 2 in the dried bicarbonate process.

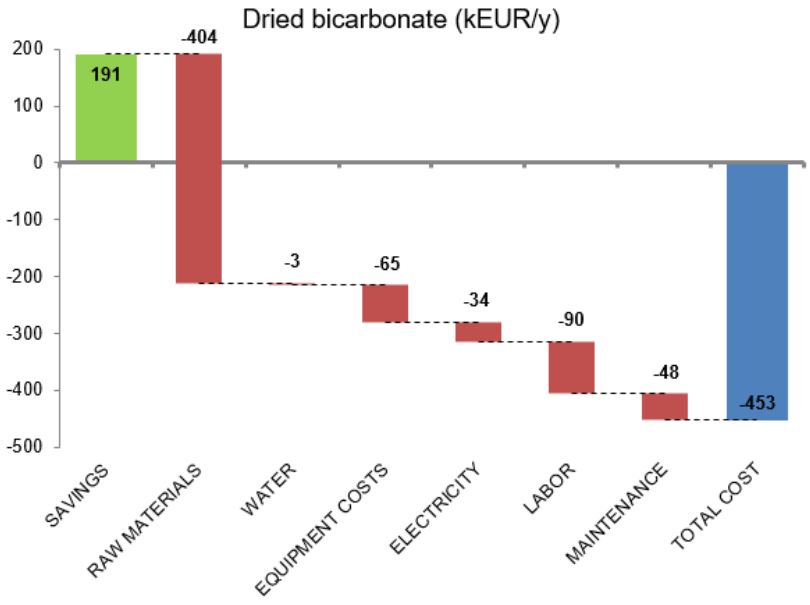

Figure 18. Waterfall chart of the dried bicarbonate sub-scenario annual costs

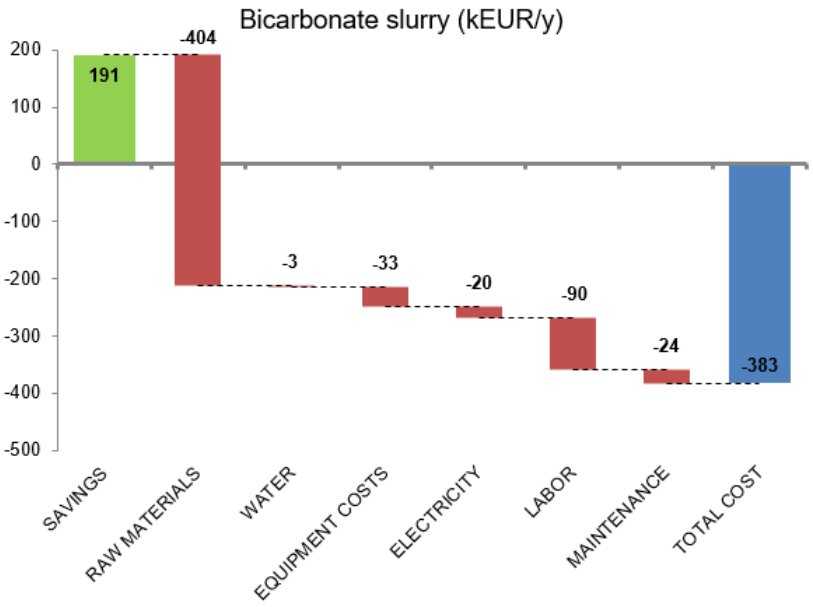

Figure 19. Waterfall chart of the bicarbonate slurry sub-scenario annual costs

The total annual cost difference is expected to be around 70 kEUR. This does not include the possible benefits of using bicarbonate in powder form, instead of a slurry. The experience of TERSA maintenance team with quicklime slurry is not very good. Thus, the two sub-scenarios could be considered viable because the cost difference is not big enough to discard any of them.

The savings of these two sub-scenarios is considered to be equal to the cost of quicklime avoided, since this is the current reagent used in the WtE plant. However, TERSA already had plans to change it to sodium bicarbonate, which has a much higher purchase price in comparison (240 EUR/t $NaHCO_3$ [63] vs 73 EUR/t CaO). Changing the savings to the cost of fresh $NaHCO_3$ avoidance compares Scenario 1, producing the bicarbonate in-house, with the direct purchase of it as a reagent. The costs difference of the two reagents is huge and sodium bicarbonate is 3.1 times more expensive than quicklime. The increase in savings (406 kEUR/y) would even outset the total cost for the bicarbonate slurry sub-scenario. Meaning that it is profitable to manufacture sodium bicarbonate in-house because its high purchase price.

Another consequence that is extracted from Figure 18 and Figure 19 is that raw material purchase cost (Na_2CO_3) accounts for 70% of the sum of costs. Thus, reducing a bit the unitary purchase price of raw materials has a big impact on the final cost figure. For example, if a good deal with the sodium carbonate producer (usually *SOLVAY*) is achieved, the total costs of operation will drop drastically.

4.2. Scenario 2: Bio-methane production

The methanation scenario includes the production of hydrogen via AEL, methanation stage which consists in three adiabatic reactors in series, and the membrane skid that recovers the carbon demanded in the methanation reaction. As explained previously, the alternative of installing PV panels on the 160 m^2 that are currently available in the TERSA plant could only produce 0.25% of the electricity demand of the electrolyzer. Thus, in terms of cost, it is not significant enough in comparison with both the AEL and methanation units. This is why it was not considered in this economic evaluation, as the PV panels cannot provide electricity at the industrial scale.

The total CAPEX of Scenario 2 is expected to be 2947 kEUR, somewhat close to 3 MEUR. This includes the membrane skid (membrane plus compressors purchase costs), methanation and bio-methane intermediate storage, and the alkaline electrolyzer unit. Figure 20 allocates the capital expenditures for the different main process units. It is clear that both AEL and methanation reaction section, which includes both de-oxo and methanation stages of Figure 12 and Figure 13, have the biggest impact on the total CAPEX of Scenario 2. However, if the point of view is shifted from the general units of electrolysis and methanation towards the pieces of equipment, the electrolyzer is the most costly equipment of the whole process. The fact that the methanation unit has several equipment (reactors, heat exchangers and vessels), whereas the electrolyzer is a stand-alone piece of equipment, makes it the most critical unit in terms of CAPEX. Moreover, AEL technology price is expected to decrease even furtherly in the near future [49], positively affecting the global CAPEX and thus increasing the benefit of the company.

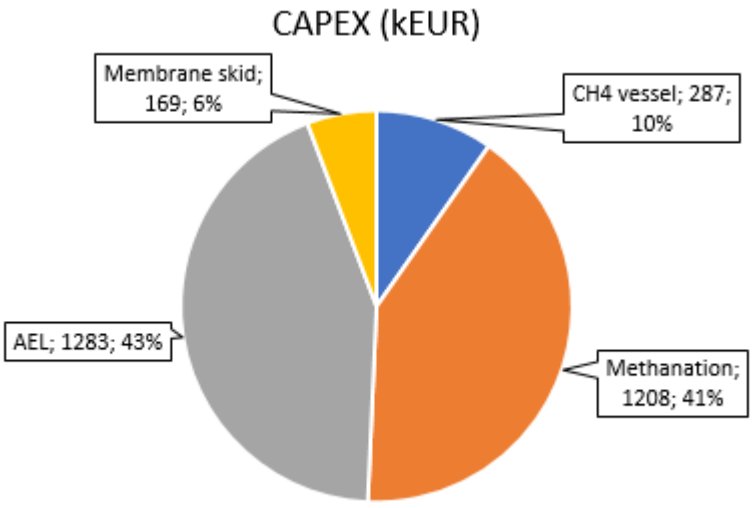

Figure 20. CAPEX allocation for Scenario 2: bio-methane production

The operational expenses of Scenario 2 are 904 kEUR/y and the biggest fraction is related to the cost of electricity. All electrolysis technologies consume a large amount of energy when breaking the water molecule. This is clearly observed in Figure 21. AEL electricity costs represent 65% of the total OPEX. In addition, if only electricity costs are taken into account, AEL demand is the 95% of this case. Although its demand is high, the current WtE plant could provide the required electricity with ease. The annual electricity demand, between the electrolyzer and membrane skid, is about 14640 MWh. In comparison with the annual electricity sold to the grid by TERSA , 171173 MWh [52], this represents an energy penalty for the WtE plant of about 9%.

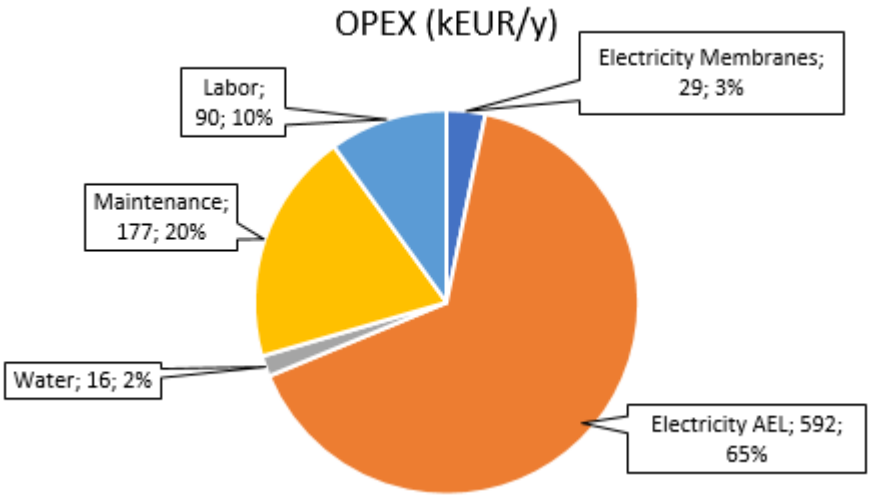

Figure 21. OPEX allocation for Scenario 2: bio-methane production

The savings of Scenario 2 come from two sources. On the one hand, the oxygen produced in the AEL is expected to be sold at a market price of 150 EUR/t [37], which in total would mean annual earnings of about 220 kEUR. On the other hand, since bio-methane produced in-house substitutes the current purchase of natural gas, the avoidance of natural gas is taken into account to compare this scenario with the status quo. Natural gas avoidance savings are calculated to be 297 kEUR/y if the current natural gas purchase price of 0.55 EUR/Nm^3 is frozen.

Spain has one of the cheapest import costs of natural gas across Europe [64]. The average kilowatt-hour price for non-household consumers after taxes in Spain on the second semester of year 2020 was 0.0284, well below the EU average of 0.033. The difference is greater in comparison with its neighboring country, France, which stands at 0.0409 EUR/kWh, an increase of 69% [65]. As a consequence, every project based in Spain which substitutes natural gas will face the economic challenge of a low natural gas price. In this case study, the low natural gas price could also be seen as an opportunity because it will probably increase in the midterm. New regulations favoring green fuels may arise in form of taxes for the traditional fossil fuels. Any increase in these costs, would increase the savings associated with producing a substitute of natural gas (SNG) in-house.

After annualizing the CAPEX using the CRF in Equation (25), the cost summary was synthetized in Figure 22. Electricity cost has the biggest impact on the annual cost standing at 54% of the total. Furtherly, if only AEL electrical consumption is considered (95% of total electricity), it represents as much as 52% of the grand total. There is not much room for improvement in the electricity price because it is already self-supplied from the WtE plant. Since the market cost will be higher than it, if sale profits are considered. Besides from the price, one way of decreasing the electricity consumption could be installing more efficient electrolyzers. Currently, AEL and PEMEL have similar efficiencies around 70%. However, the next generation SOEL could make a step further increasing the overall efficiency, as it was shown in Table 6. At the moment, the CAPEX of SOEL is too big to be considered and it is technologically not mature enough.

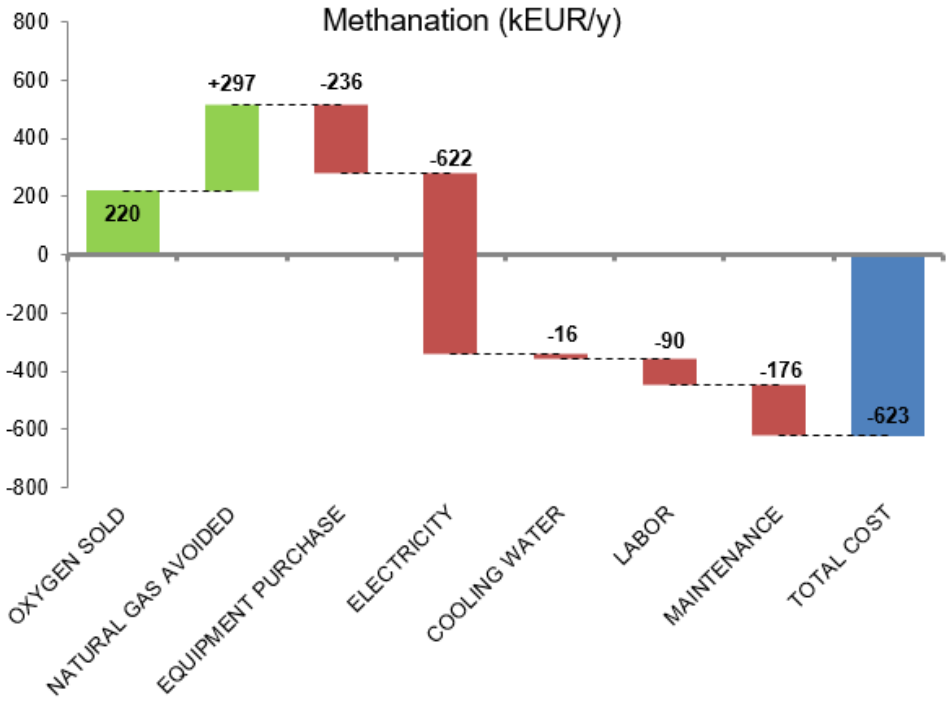

Figure 22. Waterfall chart of annual costs for Scenario 2: bio-methane production

If the cost cannot be furtherly reduced, another way of the reducing the total losses is increasing the savings in comparison with the base case. Besides natural gas, the sale price of oxygen could be increased. For example, its final application is upgraded from industry to medicine. Purity of oxygen produced by electrolysis is very high and could meet with strict standards that are paid accordingly.

4.3. Additional feasibility studies. Expander and PV panels

Once Scenarios 1 and 2 results have been discussed, the results of installing an expander in the carbon capture stage and PV panels to feed the electrolyzer are discussed below.

4.3.1. Membrane separation optimization. Expander

The expander recovers energy from the retentate stream that is vented to the atmosphere. This stream is considered as waste. The pressure difference between 7.2 bar to 1 bar drives the expander. The initial investment of the membrane system is higher because of the expander's additional cost. However, since the electricity demand is lower, electricity savings accumulate each year. Figure 23 shows the net cost flow of the carbon capture with and without an expander. The required inlet raw flue gases flowrate that meets the CO_2 demand of the bicarbonate and methanation scenarios were the base for this comparison.

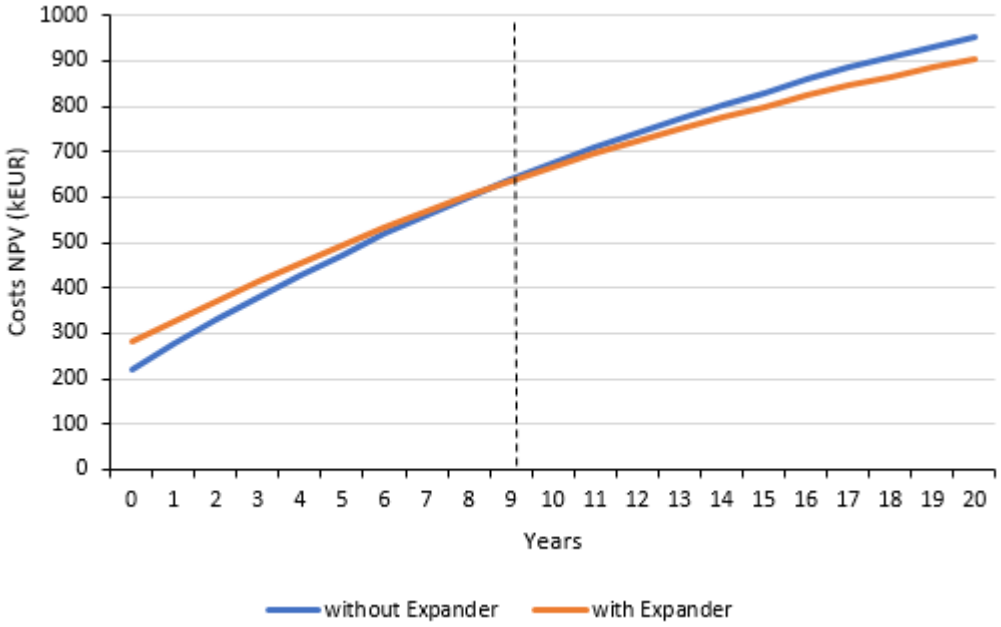

Figure 23. Payback time analysis of an expander

The payback time of installing an expander to recover part of the energy was 9 years approximately. The increase on the initial capital expenditure is offset by the electricity savings. Then, it is recommended to invest in the expander because it will report benefits in the future.

4.3.2. PV panels

The energy that the installed PV panels on the 160 m^2 of available surface in the existing WtE plant provide is insignificant in comparison with the electrolyzer demand. According to the PVSyst simulation, the solar cells could only produce 33520 kWh annually, which represents the 0.25% of the electrolyzer demand. Thus, if the plant cannot be expanded to gain terrain to install more PV, using solar energy to produce hydrogen does not report any remarkable economic benefit.

However, the PV panels could be used to supply energy to the TERSA offices located in the same facility. Figure 24 shows the payback period of this investment. The PV panels cost, assuming an electrical consumption of 33520 kWh/y, is amortized after 10 years.

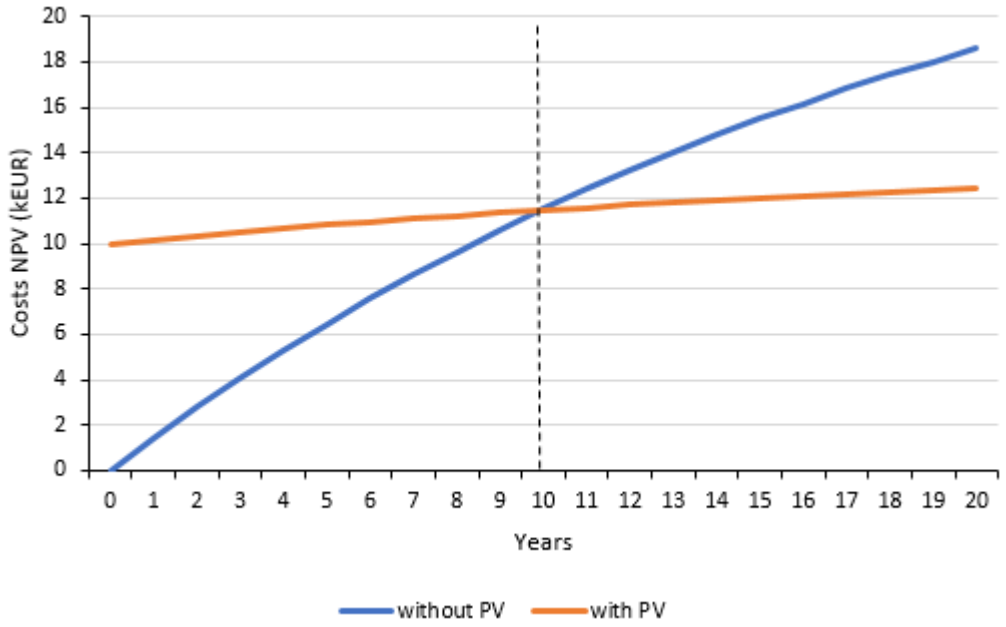

Figure 24. Payback time analysis of PV panels

The main factor making PV panels a good investment is its very low OPEX. This brief analysis shows that it is worth installing them for common self-consumption uses, such as offices. Their application at the industrial scale needs lots of land. In the case of TERSA, which already produces low-carbon energy from MSW, there are not enough reasons to install PV panels just for industrial purposes.

4.4. Bicarbonate + Bio-methane production

When both bicarbonate and methanation scenarios are considered at the same time, the process units that come after the carbon capture stage remain unchanged. Carbonation tower, drying and centrifuging, water electrolysis and methanation steps mass and energy balances are independent between them. Then, their respective cost was summed to obtain the grand total. In contrast, carbon capture with membranes is a shared unit which feeds the downstream processes. The total CO_2 demand is the sum of the previous two routes demand. The design equations for this common section are not linear and, thus, the resulting skid is not scaled up linearly and neither do the costs. Because of the economies of scale, the costs of this overall scenario are slightly lower than the direct sum of the scenarios 1 and 2. The results of the new simulation are shown in Figure 25. The overall scenario is 3 kEUR/y cheaper than adding the costs of the methanation and dry bicarbonate scenarios.

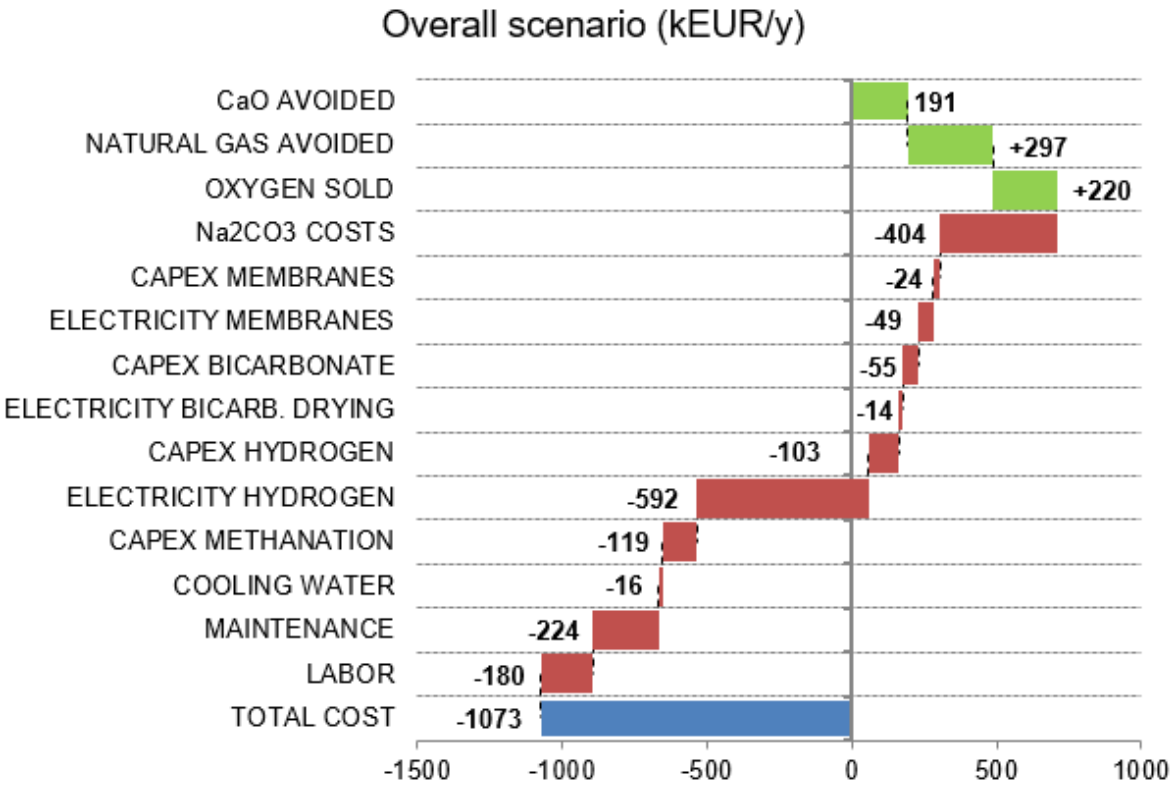

Figure 25. Waterfall chart of the overall scenario annual costs

The costs that have the biggest weight are the leading ones of each scenario: sodium carbonate purchase costs and electrical demand for the electrolyzer. For the sake of simplicity, the total CAPEX and OPEX of the methanation and bicarbonate (dry and slurry) scenarios are shown in Table 22.

Table 22. CAPEX, OPEX and savings from Scenarios 1 and 2

	1. Bicarbonate		**2. Bio-methane**
	Dry bicarbonate	Bicarbonate slurry	
CAPEX (kEUR)	1022	434	2947
OPEX (kEUR/y)	579	541	904
Savings (kEUR/y)	191	191	517
Total annual costs (kEUR/y)	453	383	624

Although producing bio-methane in-house reports the biggest savings in comparison with Scenario 1 (bicarbonate scenarios), the capital and operation costs of the electrolyzer are too high. As a consequence, Scenario 2 (bio-methane) ends up being the most expensive in terms of annual costs.

When comparing the bicarbonate sub-scenarios, the savings are the same because the same amount of quicklime is avoided. However, the bigger costs of the drying operation make the dry sub-scenario the more expensive between them. Nevertheless, revenues were not expected to be made because the goal of this case study has been optimizing and self-supplying the current TERSA plant.

Going back to the note of section 3.4 Carbon Capture with membrane technology regarding the possibility of not separating the CO_2 from the flue gases, the expected main costs differences are:

- Avoidance of membrane CAPEX (24 kEUR/y) and OPEX (49 kEUR/y).
- Increase of carbonation tower CAPEX (55 kEUR/y)
- Increase of methanation CAPEX (119 kEUR/y)
- Increase of compression costs

The costs for each item are in brackets according to Figure 25. The maximum savings expected are around 73 kEUR/y. When it comes to the increase of CAPEX, it is harder to estimate. However, if the CO_2 concentration without carbon capture is 8.78 %(v), the flowrate shall increase by a factor higher than 10. As a consequence, the methanation and carbonation equipment will work with a flowrate 10 times bigger, drastically increasing the capex according to the six-tenths rule. Therefore, it is expected that working with direct methanation and carbonation would lead to higher total costs.

Once the final economic results have been obtained, it is the duty of the company to decide whether the inversion is worth the environmental benefits of having a closer supply chain or not. The scope of this work is concluded with the bio-methane and bicarbonate (dry and slurry) scenarios being technically acceptable. Furthermore, the commercial tabulation of Table 22 gives an approximate of the total costs of each scenario.

5. Conclusions

A conceptual design of a revamp Project for the TERSA WtE plant in Sant Adrià del Besós was carried out in this work. The study included a techno-economic evaluation of two new possible process scenarios to manufacture new products. Sodium bicarbonate and bio-methane production pathways from captured carbon dioxide were pre-selected by the company and furtherly developed in this study. Both technical and economic data provided by TERSA were used to estimate the costs as close to reality as possible. The results obtained are a specific case study for a general problem that all WtE plant around the world have in common, the use of an acid gas cleaning reagent and natural gas to fire up the furnaces.

During the formulation of the mass balance, it was demonstrated that the different process routes proposed are technically feasible. Moreover, all process technologies are mature enough and have references for similar existing industrial-scale plants. The WtE emits and produces enough carbon dioxide, heat and electricity to satisfy the new units' requirements. Thus, the overall plant will be self-sufficient if the new process units are constructed, with the only exception being the supply of a new raw material, sodium carbonate.

TERSA, as a public owned company, does not make any economic profit from its activity. All revenues are reinvested to optimize the same plant and giving a better waste treatment solution for the AMB citizens. The statement of not selling product was taken into account and only oxygen is expected to be sold as a secondary by-product. As a consequence, the economic evaluation shows that Scenario 1 (bicarbonate) costs 453 kEUR/y in its dry form and 383 kEUR/y in 35%wt slurry format, and Scenario 2 (bio-methane) 623 kEUR/y.

After the closure of this conceptual techno-economic evaluation, the results obtained for both the sodium bicarbonate and bio-methane scenarios are attractive enough to be taken to a Gate Review. If TERSA approves the process concept of this proposal, the Project could move on to the next design phase: Basic Engineering or pre-FEED (Front End Engineering Design).

References

[1] "Paris Agreement | Climate Action." https://ec.europa.eu/clima/policies/international/negotiations/paris_en (accessed May 29, 2021).

[2] "Progress made in cutting emissions | Climate Action." https://ec.europa.eu/clima/policies/strategies/progress_en (accessed May 29, 2021).

[3] M. Haaf, R. Anantharaman, S. Roussanaly, J. Ströhle, and B. Epple, "CO2 capture from waste-to-energy plants: Techno-economic assessment of novel integration concepts of calcium looping technology," *Resour. Conserv. Recycl.*, vol. 162, no. July, p. 104973, 2020, doi: 10.1016/j.resconrec.2020.104973.

[4] "Landfill waste." https://ec.europa.eu/environment/topics/waste-and-recycling/landfill-waste_en (accessed May 29, 2021).

[5] "File:Waste treatment by type of recovery and disposal, 2018 (% of total treatment) 30-04-2021.png - Statistics Explained." https://ec.europa.eu/eurostat/statistics-explained/index.php?title=File:Waste_treatment_by_type_of_recovery_and_disposal,_2018_(%25_of_total_treatment)_30-04-2021.png (accessed May 29, 2021).

[6] H. J. Ho, A. Iizuka, and E. Shibata, "Carbon Capture and Utilization Technology without Carbon Dioxide Purification and Pressurization: A Review on Its Necessity and Available Technologies," *Ind. Eng. Chem. Res.*, vol. 58, no. 21, pp. 8941–8954, 2019, doi: 10.1021/acs.iecr.9b01213.

[7] "Vídeo de la Planta Integral de Valorización de Residuos (PIVR) de Sant Adrià de Besòs en English - YouTube." https://www.youtube.com/watch?v=_oFcWET3ScM&ab_channel=GrupTERSAGrupTERSA (accessed Jun. 05, 2021).

[8] "Grupo Tersa." https://www.tersa.cat/es-es/actualitat/grup-tersa-posa-en-marxa-l-innovador-sistema-catalític-a-la-planta-de-valorització-energètica-que-permet-una-reducció-d-emissions-de-fins-a-un-50/ (accessed Jun. 05, 2021).

[9] "Ecoparc3.net." https://ecoparc3.net/ (accessed Jun. 05, 2021).

[10] J. Lui, W. H. Chen, D. C. W. Tsang, and S. You, "A critical review on the principles, applications, and challenges of waste-to-hydrogen technologies," *Renew. Sustain. Energy Rev.*, vol. 134, no. August, p. 110365, 2020, doi: 10.1016/j.rser.2020.110365.

[11] H. Mikulčić *et al.*, "Flexible Carbon Capture and Utilization technologies in future energy systems and the utilization pathways of captured CO2," *Renew. Sustain. Energy Rev.*, vol. 114, no. January, 2019, doi: 10.1016/j.rser.2019.109338.

[12] P. Wienchol, A. Szlęk, and M. Ditaranto, "Waste-to-energy technology integrated with carbon capture – Challenges and opportunities," *Energy*, vol. 198, 2020, doi: 10.1016/j.energy.2020.117352.

[13] Y. Duan, L. Duan, J. Wang, and E. John, “Observation of simultaneously low CO , NO x and SO 2 emission during oxy- coal combustion in a pressurized fluidized bed,” *Fuel*, vol. 242, no. October 2018, pp. 374–381, 2019, doi: 10.1016/j.fuel.2019.01.048.

[14] M. Ostrycharczyk, K. Krochmalny, M. Czerep, and H. Pawlak-kruczek, “Examinations of the sulfur emission from pulverized lignite fuel , under pyrolysis and oxy-fuel combustion condition,” *Fuel*, vol. 241, no. November 2018, pp. 579–584, 2019, doi: 10.1016/j.fuel.2018.11.110.

[15] I. Ali, X. Gou, Q. Zhang, J. Wu, E. Wang, and Y. Liu, “Experimental study on NO x emission characteristics of oxy-biomass combustion,” *J. Clean. Prod.*, vol. 199, no. x, pp. 400–410, 2018, doi: 10.1016/j.jclepro.2018.07.022.

[16] D. Y. C. Leung, G. Caramanna, and M. M. Maroto-valer, “An overview of current status of carbon dioxide capture and storage technologies,” *Renew. Sustain. Energy Rev.*, vol. 39, pp. 426–443, 2014, doi: 10.1016/j.rser.2014.07.093.

[17] J. D. Seader, E. J. Henley, and D. K. Roper, *Separation Process Principles: Chemical and Biochemical operations*, 3rd ed. Hoboken, NJ: John Wiley & Sons, Inc., 2010.

[18] X. He and M. Hägg, “Membranes for Environmentally Friendly Energy Processes,” no. x, pp. 706–726, 2012, doi: 10.3390/membranes2040706.

[19] M. Yuan, H. Teichgraeber, J. Wilcox, and A. R. Brandt, “Design and operations optimization of membrane-based flexible carbon capture,” *Int. J. Greenh. Gas Control*, vol. 84, no. December 2018, pp. 154–163, 2019, doi: 10.1016/j.ijggc.2019.03.018.

[20] M. K. Mondal, H. K. Balsora, and P. Varshney, “Progress and trends in CO 2 capture / separation technologies : A review,” *Energy*, vol. 46, no. 1, pp. 431–441, 2012, doi: 10.1016/j.energy.2012.08.006.

[21] M. Kárászová *et al.*, “Post-combustion carbon capture by membrane separation, Review,” *Sep. Purif. Technol.*, vol. 238, no. December 2019, 2020, doi: 10.1016/j.seppur.2019.116448.

[22] L. S. White, K. D. Amo, T. Wu, and T. C. Merkel, “Extended field trials of Polaris sweep modules for carbon capture,” *J. Memb. Sci.*, vol. 542, no. December 2016, pp. 217–225, 2017, doi: 10.1016/j.memsci.2017.08.017.

[23] T. Brinkmann *et al.*, “Development of CO 2 Selective Poly (Ethylene Oxide) -Based Membranes : From Laboratory to Pilot Plant Scale,” *Engineering*, vol. 3, no. 4, pp. 485–493, 2017, doi: 10.1016/J.ENG.2017.04.004.

[24] T. C. Merkel, H. Lin, X. Wei, and R. Baker, “Power plant post-combustion carbon dioxide capture: An opportunity for membranes,” *J. Memb. Sci.*, vol. 359, no. 1–2, pp. 126–139, 2010, doi: 10.1016/j.memsci.2009.10.041.

[25] M. Bui *et al.*, “Carbon capture and storage (CCS): the way forward,” vol. 11, pp. 1062–1176, 2018, doi: 10.1039/c7ee02342a.

[26] T. Wich, W. Lueke, G. Deerberg, and M. Oles, “Carbon2Chem ® -CCU as a Step Toward a Circular

Economy," vol. 7, no. January, pp. 1–14, 2020, doi: 10.3389/fenrg.2019.00162.

[27] K. Ghaib and F.-Z. Ben-Fares, "Power-to-Methane : A state-of-the-art review," *Renew. Sustain. Energy Rev.*, vol. 81, pp. 433–446, 2018, doi: 10.1016/j.rser.2017.08.004.

[28] J. de Bucy, O. Lacroix, and L. Jammes, "The potential of power-to-gas," 2016.

[29] "BOE.es - BOE-A-2018-14557 Resolución de 8 de octubre de 2018, de la Dirección General de Política Energética y Minas, por la que se modifican las normas de gestión técnica del sistema NGTS-06, NGTS-07 y los protocolos de detalle PD-01 y PD-02." https://www.boe.es/diario_boe/txt.php?id=BOE-A-2018-14557 (accessed May 31, 2021).

[30] G. Iaquaniello, S. Setini, A. Salladini, and M. De Falco, "CO2 valorization through direct methanation of flue gas and renewable hydrogen : A technical and economic assessment," *Int. J. Hydrogen Energy*, vol. 43, no. 36, pp. 17069–17081, 2018, doi: 10.1016/j.ijhydene.2018.07.099.

[31] M. Lehner, R. Tichler, and M. Koppe, *Power-to-Gas : Technology and Business Models*. Springer, 2014.

[32] M. Sterner, M. Jentsch, and U. Holzhammer, "Energiewirtschaftliche und ökologische Bewertung eines Windgas-Angebotes," Kassel, 2011.

[33] M. Bailera, P. Lisbona, L. M. Romeo, and S. Espatolero, "Power to Gas projects review : Lab , pilot and demo plants for storing renewable energy and CO 2," *Renew. Sustain. Energy Rev.*, vol. 69, no. October 2016, pp. 292–312, 2017, doi: 10.1016/j.rser.2016.11.130.

[34] F. Graf, M. Götz, M. Henel, T. Schaaf, and R. Tichler, "Abschlussbericht Technoökonomische Studie von Power-to-Gas-Konzepten," 2014. Accessed: Jun. 04, 2021. [Online]. Available: www.dvgw.de.

[35] M. Götz *et al.*, "Renewable Power-to-Gas: A technological and economic review," *Renew. Energy*, vol. 85, pp. 1371–1390, 2016, doi: 10.1016/j.renene.2015.07.066.

[36] R. K. Sinnot, *Chemical Engineering Design*, Fourth., vol. 6, no. 3. Elsevier, 2005.

[37] D. Bellotti, M. Rivarolo, L. Magistri, and A. F. Massardo, "Thermo-economic comparison of hydrogen and hydro-methane produced from hydroelectric energy for land transportation," *Int. J. Hydrogen Energy*, vol. 40, no. 6, pp. 2433–2444, 2015, doi: 10.1016/j.ijhydene.2014.12.066.

[38] R. Peters, M. Baltruweit, T. Grube, R. C. Samsun, and D. Stolten, "A techno economic analysis of the power to gas route," *J. CO2 Util.*, vol. 34, no. May, pp. 616–634, 2019, doi: 10.1016/j.jcou.2019.07.009.

[39] G. A. Olah, A. Goeppert, and G. K. S. Prakash, *Beyond oil and gas: The methanol economy*. Montreal: Wiley, 2009.

[40] V. Dieterich, A. Buttler, A. Hanel, H. Spliethoff, and S. Fendt, "Power-to-liquid via synthesis of methanol, DME or Fischer–Tropsch-fuels: a review," *Energy Environ. Sci.*, vol. 13, no. 10, pp.

3207–3252, 2020, doi: 10.1039/d0ee01187h.

[41] D. Bellotti, M. Rivarolo, L. Magistri, and A. F. Massardo, “Feasibility study of methanol production plant from hydrogen and captured carbon dioxide,” *J. CO2 Util.*, vol. 21, no. April, pp. 132–138, 2017, doi: 10.1016/j.jcou.2017.07.001.

[42] M. Rivarolo, D. Bellotti, L. Magistri, and A. F. Massardo, “Feasibility study of methanol production from different renewable sources and thermo-economic analysis,” *Int. J. Hydrogen Energy*, vol. 41, no. 4, pp. 2105–2116, 2016, doi: 10.1016/j.ijhydene.2015.12.128.

[43] D. Ravikumar, G. Keoleian, and S. Miller, “The environmental opportunity cost of using renewable energy for carbon capture and utilization for methanol production,” *Appl. Energy*, vol. 279, no. August, p. 115770, 2020, doi: 10.1016/j.apenergy.2020.115770.

[44] P. Huttenhuis, A. Roeloffzen, and G. Versteeg, “CO2 capture and re-use at a waste incinerator,” in *Energy Procedia*, Jan. 2016, vol. 86, pp. 47–55, doi: 10.1016/j.egypro.2016.01.006.

[45] J. H. Lee, D. W. Lee, C. Kwak, K. Kang, and J. H. Lee, “Technoeconomic and environmental evaluation of sodium bicarbonate production using co2 from flue gas of a coal-fired power plant,” *Ind. Eng. Chem. Res.*, vol. 58, no. 34, pp. 15533–15541, 2019, doi: 10.1021/acs.iecr.9b02253.

[46] L. Bonfim-Rocha, A. B. Silva, S. H. B. De Faria, M. F. Vieira, and M. De Souza, “Production of Sodium Bicarbonate from CO2 Reuse Processes: A Brief Review,” *Int. J. Chem. React. Eng.*, vol. 18, no. 1, pp. 1–16, 2020, doi: 10.1515/ijcre-2018-0318.

[47] J. R. Morante, T. Andre, G. García, A. Tarancón, and M. Torrell, *Hidrógeno. Vector energético de una economía descarbonizada*, 2nd ed. IREC, 2020.

[48] A. Buttler and H. Spliethoff, “Current status of water electrolysis for energy storage, grid balancing and sector coupling via power-to-gas and power-to-liquids: A review,” *Renewable and Sustainable Energy Reviews*, vol. 82. Elsevier Ltd, pp. 2440–2454, Feb. 01, 2018, doi: 10.1016/j.rser.2017.09.003.

[49] O. Schmidt, A. Gambhir, I. Staffell, A. Hawkes, J. Nelson, and S. Few, “Future cost and performance of water electrolysis: An expert elicitation study,” *Int. J. Hydrogen Energy*, vol. 42, no. 52, pp. 30470–30492, Dec. 2017, doi: 10.1016/j.ijhydene.2017.10.045.

[50] R. Turton, R. C. Bailie, W. B. Whiting, J. A. Shaeiwitz, and D. Bhattacharyya, *Analysis, Synthesis, and Design of Chemical Processes*, 3rd ed. Pearson Education, 2009.

[51] E. Adu, Y. D. Zhang, D. Liu, and P. Tontiwachwuthikul, “Parametric process design and economic analysis of post-combustion CO2 capture and compression for coal- And natural gas-fired power plants,” *Energies*, vol. 13, no. 10, 2020, doi: 10.3390/en13102519.

[52] TERSA, “Informe de producció,” 2019.

[53] D. J. L. Savary, “Sodium bicarbonate particles manufactured by atomization,” WO2014096457, 2014.

[54] A. Tinson, S. D'Uva, J. Hu, and J. Lefas, "Process for preparing ultra HNE sodium bicarbonate powder," 2007.

[55] Solvay, "'Flue gas cleaning in Waste to Energy plants' Webinar : Key facts and Case studies," 2020. https://channel.royalcast.com/solvay/#!/solvay/20201001_1 (accessed May 06, 2021).

[56] Church & Dwight CO, "Sodium Bicarbonate, Industrial Grade Specifications." https://jcarpenterenvironmental.com/pdf/CD_Sorbent_Industrial.pdf (accessed May 07, 2021).

[57] D. Bonaventura, R. Chacartegui, J. M. Valverde, J. A. Becerra, and V. Verda, "Carbon capture and utilization for sodium bicarbonate production assisted by solar thermal power," *Energy Convers. Manag.*, vol. 149, pp. 860–874, Oct. 2017, doi: 10.1016/j.enconman.2017.03.042.

[58] J. Proost, "State-of-the art CAPEX data for water electrolysers, and their impact on renewable hydrogen price settings," *Int. J. Hydrogen Energy*, vol. 44, no. 9, pp. 4406–4413, Feb. 2019, doi: 10.1016/j.ijhydene.2018.07.164.

[59] TERSA and Ajuntament de Barcelona, "AjBCN-Xarxa fotovoltaica amb connexió a la xarxa elèctrica." https://www.google.com/maps/d/u/0/viewer?mid=1IKOXPNGoI_us1Juke5PoLZHu3ms&ll=41.408571111427946%2C2.144829706445206&z=12 (accessed May 18, 2021).

[60] "Tarifas de suministro - Web oficial - La gestió responsable." https://www.aiguesdebarcelona.cat/es/web/guest/servicio-agua/factura-y-tarifas-agua/tarifas-de-suministro (accessed Jun. 04, 2021).

[61] E. Vartiainen, G. Masson, C. Breyer, D. Moser, and E. Román Medina, "Impact of weighted average cost of capital, capital expenditure, and other parameters on future utility-scale PV levelised cost of electricity," *Prog. Photovoltaics Res. Appl.*, vol. 28, no. 6, pp. 439–453, 2020, doi: 10.1002/pip.3189.

[62] J. Xu *et al.*, "Post-combustion CO2 capture with membrane process: Practical membrane performance and appropriate pressure," *J. Memb. Sci.*, vol. 581, pp. 195–213, Jul. 2019, doi: 10.1016/j.memsci.2019.03.052.

[63] M. Rumayor, A. Dominguez-Ramos, and A. Irabien, "Toward the Decarbonization of Hard-To-Abate Sectors: A Case Study of the Soda Ash Production," *ACS Sustain. Chem. Eng.*, vol. 8, no. 32, pp. 11956–11966, Aug. 2020, doi: 10.1021/acssuschemeng.0c01598.

[64] J. Guilera, J. R. Morante, and T. Andreu, "Economic viability of SNG production from power and CO2," *Energy Convers. Manag.*, vol. 162, no. January, pp. 218–224, 2018, doi: 10.1016/j.enconman.2018.02.037.

[65] Eurostat, "Gas prices for non-household consumers - bi-annual data," 2020. https://ec.europa.eu/eurostat/databrowser/view/nrg_pc_203/default/table?lang=en (accessed May 24, 2021).

A. Annex

This additional section contains some complementary data used during the techno-economical evaluation of the different scenarios. Its contents are the following:

- 1A1. Process conditions of flue gases at TERSA WtE plant
- 1A2. Carbon capture mass balance for the overall scenario
- 1A3. Carbon capture equipment sizing for the overall scenario
- 1A4. Carbon capture equipment sizing for Scenario 1: Bicarbonate
- 1A5. Carbon capture equipment sizing for Scenario 2: Bio-methane
- 1A6. PVSyst simulation report

A1. Process conditions of flue gases at TERSA WtE plant

Particles (mg/Nm^3)	**0.32**
NOx (mg/Nm^3)	38.75
NO (mg/Nm^3)	29.55
NO_2 (mg/Nm^3)	1.64
CO (mg/Nm^3)	15.81
HCl (mg/Nm^3)	3.46
SO_2 (mg/Nm^3)	0.94
NH_3 (mg/Nm^3)	0.98
TOC (mg/Nm^3)	1.25
HF (mg/Nm^3)	0.01
Hg (µg/Nm^3)	0.67
Flowrate (Nm^3/h)	261440
CO_2 (% vol)	8.78
O_2 (% vol)	9.99
H_2O (% vol)	18.29
Pressure (mbar)	927.38
Temperature (°C)	144.57

A2. Carbon capture mass balance for the overall scenario

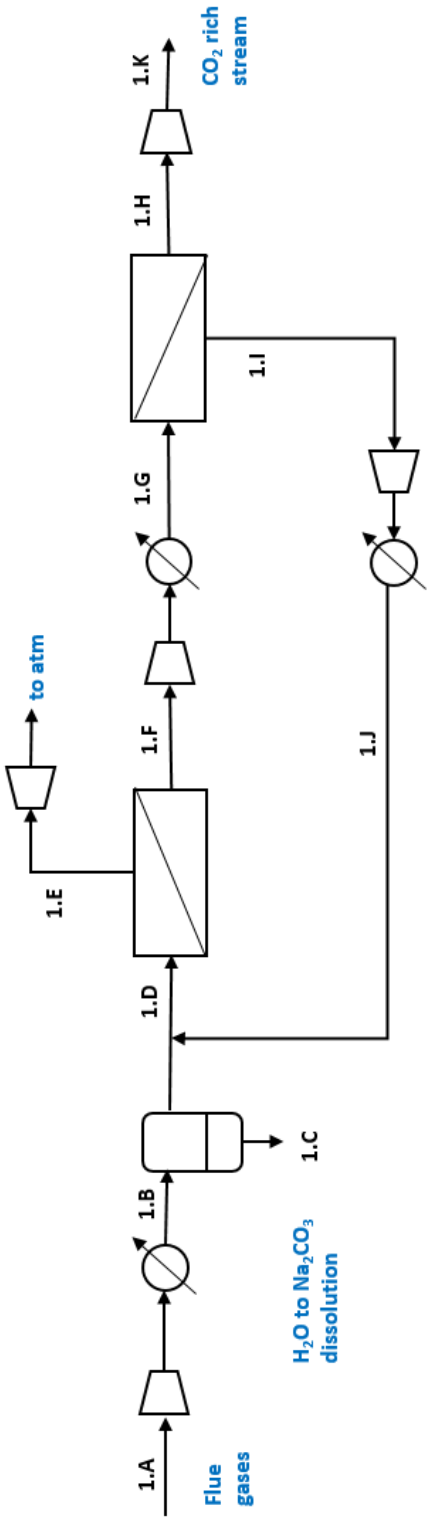

Parameter	A	B	C	D	E	F	G	H	I	J	K	Units
	Feed	Compr. Feed	Condensate	Feed 1	Retentate 1	Permeate 1	Feed 2	Permeate 2	Retentate 2	Recirc	CO2 press	
Flowrate	1329.4	1329.4	-	1165.6	978.8	186.8	186.8	107.5	79.3	79.3	107.5	Nm^3/h
Molar Flowrate	59386.1	59386.1	10861.7	52068.0	43723.7	8344.3	8344.3	4800.6	3543.7	3543.7	4800.6	mol/h
CO2 Flowrate	5214.1	5214.1	0	5729.8	573.0	5156.8	5156.8	4641.1	515.7	515.7	4641.1	mol/h
N2 Flowrate	37377.6	37377.6	0	39620.1	37290.1	2329.9	2329.9	87.5	2242.5	2242.5	87.5	mol/h
O2 Flowrate	5932.7	5932.7	0	6718.2	5860.7	857.5	857.5	72.0	785.5	785.5	72.0	mol/h
H2O Flowrate	10861.7	10861.7	10861.7	0.0	0.0	0.0	0.0	0.0	0.0	0.0	0.0	mol/h
X CO2	0.0878	0.0878	0.0000	0.1100	0.0131	0.6180	0.6180	0.9668	0.1455	0.1455	0.9668	-
X N2	0.6294	0.6294	0.0000	0.7609	0.8529	0.2792	0.2792	0.0182	0.6328	0.6328	0.0182	-
X O2	0.0999	0.0999	0.0000	0.1290	0.1340	0.1028	0.1028	0.0150	0.2217	0.2217	0.0150	-
X H2O	0.1829	0.1829	1.0000	0.0000	0.0000	0.0000	0.0000	0.0000	0.0000	0.0000	0.0000	-
T	420	311	311	311	311	311	311	311	311	311	311.0	K
P	1.00	8.00	8.00	8.00	7.20	1.00	3.00	1.00	2.70	8.00	5.00	bar

A3. Carbon capture equipment sizing for the overall scenario

Parameter	Value
Feed flowrate (Nm^3/h)	1329
CO_2 production (Nm^3/h)	103.9
Membrane 1 area (m^2)	81.5
Membrane 2 area (m^2)	21.7
Compressor 1 duty (kW)	170
Compressor 2 duty (kW)	8
Compressor 3 duty (kW)	3
Compressor 4 duty (kW)	7
Expander duty (kW)	29

A4. Carbon capture equipment sizing for Scenario 1: Bicarbonate

Parameter	Value
Feed flowrate (Nm^3/h)	538
CO_2 production (Nm^3/h)	42.1
Membrane 1 area (m^2)	33.0
Membrane 2 area (m^2)	8.8
Compressor 1 duty (kW)	69
Compressor 2 duty (kW)	3
Compressor 3 duty (kW)	1
Compressor 4 duty (kW)	3
Expander duty (kW)	12

A5. Carbon capture equipment sizing for Scenario 2: Bio-methane

Parameter	Value
Feed flowrate (Nm^3/h)	791
CO_2 production (Nm^3/h)	61.8
Membrane 1 area (m^2)	48.5
Membrane 2 area (m^2)	12.9
Compressor 1 duty (kW)	101
Compressor 2 duty (kW)	5
Compressor 3 duty (kW)	2
Compressor 4 duty (kW)	4
Expander duty (kW)	17

A6. PVSyst simulation report

Version 7.2.2

PVsyst - Simulation report

Stand alone system

Project: Nuevo Proyecto

Variant: Nueva variante de simulación

Stand alone system with batteries

System power: 21.56 kWp

El Besòs i el Maresme - Spain

Author

PVsyst V7.2.2
VC0, Simulation date:
13/05/21 18:45
with v7.2.2

Project: Nuevo Proyecto

Variant: Nueva variante de simulación

Project summary

Geographical Site
El Besòs i el Maresme
Spain

Situation

Latitude	41.42 °N
Longitude	2.23 °E
Altitude	11 m
Time zone	UTC+1

Project settings

Albedo	0.20

Meteo data
el Besòs i el Maresme
Meteonorm 8.0 (1996-2015), Sat=29% - Sintético

System summary

Stand alone system

Stand alone system with batteries

PV Field Orientation
Fixed plane
Tilt/Azimuth 30 / 0 °

User's needs
Daily household consumers
Constant over the year
Average 3849 kWh/Day

System information

PV Array

Nb. of modules	392 units
Pnom total	21.56 kWp

Battery pack

Technology	Lithium-ion, NMC
Nb. of units	50 units
Voltage	1234 V
Capacity	14820 Ah

Results summary

Available Energy	33521 kWh/year	Specific production	1555 kWh/kWp/year	Perf. Ratio PR	93.93 %
Used Energy	37797 kWh/year			Solar Fraction SF	2.69 %

Table of contents

PVsyst V7.2.2
VC0, Simulation date:
13/05/21 18:45
with v7.2.2

Project: Nuevo Proyecto
Variant: Nueva variante de simulación

General parameters

Stand alone system — **Stand alone system with batteries**

PV Field Orientation

Orientation		Sheds configuration		Models used	
Fixed plane		No 3D scene defined		Transposition	Perez
Tilt/Azimuth	30 / 0 °			Diffuse	Perez, Meteonorm
				Circumsolar	separate

User's needs
Daily household consumers
Constant over the year
Average 3849 kWh/Day

PV Array Characteristics

PV module

Manufacturer	Generic
Model	Mono 55 Wp 36 cells
(Original PVsyst database)	
Unit Nom. Power	55 Wp
Number of PV modules	392 units
Nominal (STC)	21.56 kWp
Modules	4 Strings x 98 In series
At operating cond. (50°C)	
Pmpp	19.42 kWp
U mpp	1602 V
I mpp	12 A

Battery

Manufacturer	Generic
Model	Rack JH4 SR32_4P
Technology	Lithium-ion, NMC
Nb. of units	50 in parallel
Discharging min. SOC	10.0 %
Stored energy	16574.7 kWh
Battery Pack Characteristics	
Voltage	1234 V
Nominal Capacity	14820 Ah (C10)
Temperature	Fixed 20 °C

Controller

Universal controller	
Technology	MPPT converter
Temp coeff.	-5.0 mV/°C/Elem.
Converter	
Maxi and EURO efficiencies	97.0 / 95.0 %

Battery Management control

Threshold commands as	SOC calculation
Charging	SOC = 0.96 / 0.80
Discharging	SOC = 0.10 / 0.35

Total PV power

Nominal (STC)	22 kWp
Total	392 modules
Module area	142 m²
Cell area	56.4 m²

Array losses

Thermal Loss factor
Module temperature according to irradiance
Uc (const) 20.0 W/m²K
Uv (wind) 0.0 W/m²K/m/s

DC wiring losses
Global array res. 2228 mΩ
Loss Fraction 1.5 % at STC

Serie Diode Loss
Voltage drop 0.7 V
Loss Fraction 0.0 % at STC

Module Quality Loss
Loss Fraction -0.8 %

Module mismatch losses
Loss Fraction 2.0 % at MPP

Strings Mismatch loss
Loss Fraction 0.1 %

IAM loss factor
Incidence effect (IAM): Fresnel smooth glass, n = 1.526

0°	30°	50°	60°	70°	75°	80°	85°	90°
1.000	0.998	0.981	0.948	0.862	0.776	0.636	0.403	0.000

PVsyst V7.2.2
VC0, Simulation date:
13/05/21 18:45
with v7.2.2

Detailed User's needs

Daily household consumers, Constant over the year, average = 3849 kWh/day

Annual values

	Number	Power	Use	Energy
		W	Hour/day	Wh/day
Lavaplatos y lavadora	1		24	3849360
Consumidores en espera			24.0	24
Total daily energy				3849384Wh/day

Hourly distribution

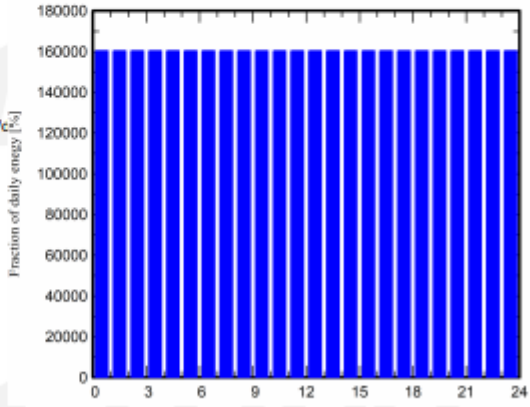

PVsyst V7.2.2
VC0, Simulation date:
13/05/21 18:45
with v7.2.2

Project: Nuevo Proyecto

Variant: Nueva variante de simulación

Main results

System Production

Available Energy	33521 kWh/year	Specific production	1555 kWh/kWp/year
Used Energy	37797 kWh/year	Performance Ratio PR	93.93 %
Excess (unused)	0 kWh/year	Solar Fraction SF	2.69 %
Loss of Load		**Battery aging (State of Wear)**	
Time Fraction	97.3 %	Cycles SOW	100.0 %
Missing Energy	1367228 kWh/year	Static SOW	80.0 %

Normalized productions (per installed kWp)

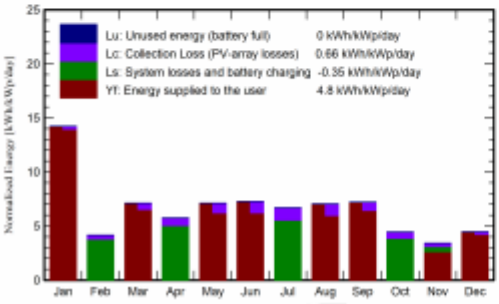

Performance Ratio PR

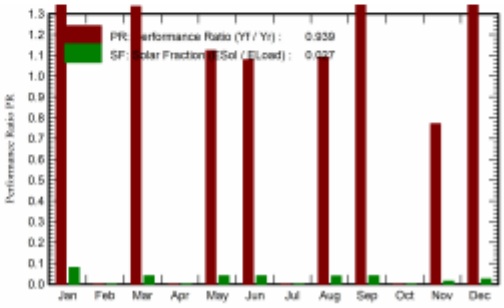

Balances and main results

	GlobHor kWh/m²	GlobEff kWh/m²	E_Avail kWh	EUnused kWh	E_Miss kWh	E_User kWh	E_Load kWh	SolFrac ratio
January	63.7	107.6	2092	0.000	109816	9515	119331	0.080
February	80.3	113.6	2198	0.000	107783	0	107783	0.000
March	130.7	160.9	3041	0.000	114578	4753	119331	0.040
April	157.9	168.0	3135	0.091	115482	0	115482	0.000
May	196.1	190.6	3474	0.000	114574	4757	119331	0.040
June	209.8	196.1	3518	0.088	110778	4704	115482	0.041
July	212.0	201.1	3550	0.000	119331	0	119331	0.000
August	186.8	194.6	3440	0.091	114617	4714	119331	0.040
September	136.5	156.5	2847	0.091	110816	4666	115482	0.040
October	100.7	134.4	2474	0.000	119331	0	119331	0.000
November	65.3	99.8	1924	0.000	113781	1701	115482	0.015
December	54.8	93.4	1827	0.000	116343	2988	119331	0.025
Year	1594.7	1816.7	33521	0.361	1367228	37797	1405025	0.027

Legends

GlobHor	Global horizontal irradiation	E_User	Energy supplied to the user
GlobEff	Effective Global, corr. for IAM and shadings	E_Load	Energy need of the user (Load)
E_Avail	Available Solar Energy	SolFrac	Solar fraction (EUsed / ELoad)
EUnused	Unused energy (battery full)		
E_Miss	Missing energy		

PVsyst V7.2.2
VC0, Simulation date:
13/05/21 18:45
with v7.2.2

Project: Nuevo Proyecto

Variant: Nueva variante de simulación

Loss diagram